

References

References

1. Zhao, C. M. *et al.* TBX20 loss-of-function mutation associated with familial dilated cardiomyopathy. *Clin Chem Lab Med* **54**, 325–332 (2016).
2. Chakraborty, S. & Yutzey, K. E. Tbx20 regulation of cardiac cell proliferation and lineage specialization during embryonic and fetal development in vivo. *Dev Biol* **363**, 234–246 (2012).
3. Kirk, E. P. *et al.* Mutations in cardiac T-box factor gene TBX20 are associated with diverse cardiac pathologies, including defects of septation and valvulogenesis and cardiomyopathy. *Am J Hum Genet* **81**, 280–291 (2007).
4. Chakraborty, S., Sengupta, A. & Yutzey, K. E. Journal of Molecular and Cellular Cardiology Tbx20 promotes cardiomyocyte proliferation and persistence of fetal characteristics in adult mouse hearts. *J Mol Cell Cardiol* **62**, 203–213 (2013).
5. Shen, T. *et al.* Tbx20 functions as an important regulator of estrogen-mediated cardiomyocyte protection during oxidative stress. *Int J Cardiol* **168**, (2013).
6. Sen, P., Polley, A., Sengupta, A. & Chakraborty, S. Tbx20 promotes H9c2 cell survival against oxidative stress and hypoxia in vitro. **57**, 643–655 (2019).
7. Stennard, F. A. *et al.* Cardiac T-box factor Tbx20 directly interacts with Nkx2-5, GATA4, and GATA5 in regulation of gene expression in the developing heart. *Dev Biol* **262**, 206–224 (2003).
8. Wang, H. *et al.* Nkx2-5 Regulates the Proliferation and Migration of H9c2 Cells. *Med Sci Monit* **26**, e925388 (2020).
9. Kanamori, H. *et al.* Functional significance and morphological characterization of starvation-induced autophagy in the adult heart. *American Journal of Pathology* **174**, 1705–1714 (2009).
10. Xu, X., Pacheco, B. D., Leng, L., Bucala, R. & Ren, J. Macrophage migration inhibitory factor plays a permissive role in the maintenance of cardiac contractile function under starvation through regulation of autophagy. *Cardiovasc Res* **99**, 412–421 (2013).

11. Moulis, M. & Vindis, C. Methods for Measuring Autophagy in Mice. **1**, 1–14 (2017).
12. Schiaffino, S., Mammucari, C. & Sandri, M. The role of autophagy in neonatal tissues: Just a response to amino acid starvation? *Autophagy* vol. 4 727–730 Preprint at <https://doi.org/10.4161/auto.6143> (2008).
13. Wang, X., Guo, Z., Ding, Z. & Mehta, J. L. Inflammation, Autophagy, and Apoptosis After Myocardial Infarction. (2018) doi:10.1161/JAHA.117.008024.
14. Kanamori, H. *et al.* The role of autophagy emerging in postinfarction cardiac remodelling. 330–339 (2018) doi:10.1093/cvr/cvr073.
15. Ma, S., Wang, Y., Chen, Y. & Cao, F. The role of the autophagy in myocardial ischemia/reperfusion injury. *Biochimica et Biophysica Acta - Molecular Basis of Disease* vol. 1852 271–276 Preprint at <https://doi.org/10.1016/j.bbadis.2014.05.010> (2015).
16. Kanamori, H. *et al.* Autophagy limits acute myocardial infarction induced by permanent coronary artery occlusion. *Am J Physiol Heart Circ Physiol* **300**, 2261–2271 (2011).
17. Wu, X. *et al.* Impaired Autophagy Contributes to Adverse Cardiac Remodeling in Acute Myocardial Infarction. **9**, 1–11 (2014).
18. Rubinsztein, D. C., Mariño, G. & Kroemer, G. Autophagy and aging. *Cell* vol. 146 682–695 Preprint at <https://doi.org/10.1016/j.cell.2011.07.030> (2011).
19. Abdellatif, M., Sedej, S., Carmona-Gutierrez, D., Madeo, F. & Kroemer, G. Autophagy in cardiovascular aging. *Circ Res* **123**, 803–824 (2018).
20. Sciarretta, S., Maejima, Y., Zablocki, D. & Sadoshima, J. The Role of Autophagy in the Heart. *The Annual Review of Physiology is online at* **80**, 1–26 (2018).
21. D’Onofrio, N., Servillo, L. & Balestrieri, M. L. SIRT1 and SIRT6 Signaling Pathways in Cardiovascular Disease Protection. *Antioxidants and Redox Signaling* vol. 28 711–732 Preprint at <https://doi.org/10.1089/ars.2017.7178> (2018).

22. Ministrini, S. *et al.* Sirtuin 1 in Endothelial Dysfunction and Cardiovascular Aging. *Frontiers in Physiology* vol. 12 Preprint at <https://doi.org/10.3389/fphys.2021.733696> (2021).
23. Winnik, S., Auwerx, J., Sinclair, D. A. & Matter, C. M. Protective effects of sirtuins in cardiovascular diseases: From bench to bedside. *European Heart Journal* vol. 36 3404–3412 Preprint at <https://doi.org/10.1093/eurheartj/ehv290> (2015).
24. Gao, G. *et al.* Rapamycin regulates the balance between cardiomyocyte apoptosis and autophagy in chronic heart failure by inhibiting mTOR signaling. *Int J Mol Med* **45**, 195–209 (2020).
25. Yamaguchi, O. Autophagy in the heart. *Circulation Journal* **83**, 697–704 (2019).
26. Maiese, K. The mechanistic target of rapamycin (mTOR) and the silent mating-type information regulation 2 homolog 1 (SIRT1): oversight for neurodegenerative disorders. *Biochemical Society Transactions* vol. 46 351–360 Preprint at <https://doi.org/10.1042/BST20170121> (2018).
27. Dobaczewski, M., Gonzalez-Quesada, C. & Frangogiannis, N. G. The extracellular matrix as a modulator of the inflammatory and reparative response following myocardial infarction. *J Mol Cell Cardiol* **48**, 504–511 (2010).
28. Levick, S. P. & Brower, G. L. Regulation of matrix metalloproteinases is at the heart of myocardial remodeling. **295**, 8–10 (2018).
29. Dobaczewski, M., Gonzalez-quesada, C. & Frangogiannis, N. G. Journal of Molecular and Cellular Cardiology The extracellular matrix as a modulator of the inflammatory and reparative response following myocardial infarction. *J Mol Cell Cardiol* **48**, 504–511 (2010).
30. Talman, V. & Ruskoaho, H. Cardiac fibrosis in myocardial infarction—from repair and remodeling to regeneration. *Cell Tissue Res* **365**, 563–581 (2016).
31. Berk, B. C., Fujiwara, K. & Lehoux, S. Review series ECM remodeling in hypertensive heart disease. **117**, (2007).
32. Manuscript, A. NIH Public Access. **11**, 339–346 (2010).

33. Uluçay, S. *et al.* A novel association between TGF β 1 and ADAMTS4 in coronary artery disease: A new potential mechanism in the progression of atherosclerosis and diabetes. *Anadolu Kardiyoloji Dergisi* **15**, 823–829 (2015).
34. Pengse Po¹, Erin Delaney¹, Howard Gamper², Miklos Szanti-Kis³, Lee Speight³, LiWei Tu¹, Andrey Kosolapov¹, E. James Petersson³, Ya-Ming Hou², and C. D. HHS Public Access. *Physiol Behav* **176**, 139–148 (2017).
35. Y, Y. O. Inhibition of ADAMTS4 (aggrecanase-1) by tissue inhibitors of. **494**, 192–195 (2001).
36. Vistnes, M. *et al.* Pentosan polysulfate decreases myocardial expression of the extracellular matrix enzyme ADAMTS4 and improves cardiac function in vivo in rats subjected to pressure overload by aortic banding. *PLoS One* **9**, (2014).
37. Ayanoglu, T. *et al.* The role of ADAMTS genes in the end stage of hip osteoarthritis. *Acta Orthop Traumatol Turc* **53**, 140–144 (2019).
38. Liao, L. *et al.* Acute Synovitis after Trauma Precedes and is Associated with Osteoarthritis Onset and Progression. *Int J Biol Sci* **16**, 970–980 (2020).
39. Rao, N. *et al.* ADAMTS4 and its proteolytic fragments differentially affect melanoma growth and angiogenesis in mice. *Int J Cancer* **133**, 294–306 (2013).
40. Shang, X. Q. *et al.* ADAMTS4 is upregulated in colorectal cancer and could be a useful prognostic indicator of colorectal cancer. *Rev Assoc Med Bras (1992)* **66**, 42–47 (2020).
41. Hossain, Z., Poh, K. K., Hirohata, S. & Ogawa, H. Loss of ADAMTS4 reduces high fat diet-induced atherosclerosis and enhances plaque stability in. *Nature Publishing Group* 1–15 (2016) doi:10.1038/srep31130.
42. Li, K. *et al.* Assessing serum levels of ADAMTS1 and ADAMTS4 as new biomarkers for patients with type a acute aortic dissection. *Medical Science Monitor* **23**, 3913–3922 (2017).
43. Zha, Y., Chen, Y., Xu, F. & Zhang, J. Elevated level of ADAMTS4 in plasma and peripheral monocytes from patients with acute coronary syndrome. 781–786 (2010) doi:10.1007/s00392-010-0183-1.

44. Walton, K. L., Johnson, K. E. & Harrison, C. A. Targeting TGF- β mediated SMAD signaling for the prevention of fibrosis. *Front Pharmacol* **8**, (2017).
45. Pohlers, D. *et al.* TGF- β and fibrosis in different organs - molecular pathway imprints. *Biochim Biophys Acta Mol Basis Dis* **1792**, 746–756 (2009).
46. Lou, Z. *et al.* Upregulation of NOX2 and NOX4 Mediated by TGF- β Signaling Pathway Exacerbates Cerebral Ischemia/Reperfusion Oxidative Stress Injury. *Cellular Physiology and Biochemistry* **46**, 2103–2113 (2018).
47. Frangogiannis, N. G. *Cardiac fibrosis: Cell biological mechanisms, molecular pathways and therapeutic opportunities. Molecular Aspects of Medicine* vol. 65 (2019).
48. Yang, Y. F., Wu, C. C., Chen, W. P. & Su, M. J. Transforming growth factor- β type I receptor/ALK5 contributes to doxazosin-induced apoptosis in H9C2 cells. *Naunyn Schmiedebergs Arch Pharmacol* **380**, 561–567 (2009).
49. Buijtenlijk, M. F. J., Barnett, P. & van den Hoff, M. J. B. Development of the human heart. *Am J Med Genet C Semin Med Genet* **184**, 7–22 (2020).
50. Wang, J., Liu, S., Heallen, T. & Martin, J. F. The Hippo pathway in the heart: pivotal roles in development, disease, and regeneration. *Nature Reviews Cardiology* vol. 15 672–684 Preprint at <https://doi.org/10.1038/s41569-018-0063-3> (2018).
51. Knutson, A. K., Williams, A. L., Boisvert, W. A. & Shohet, R. V. HIF in the heart: Development, metabolism, ischemia, and atherosclerosis. *Journal of Clinical Investigation* vol. 131 Preprint at <https://doi.org/10.1172/JCI137557> (2021).
52. Firulli, A. B. & Thattaliyath, B. D. *Transcription Factors in Cardiogenesis: The Combinations That Unlock the Mysteries of the Heart. Inremotioml Review of Cytology* vol. 214.
53. Stennard, F. A. & Harvey, R. P. T-box transcription factors and their roles in regulatory hierarchies in the developing heart. *Development* vol. 132 4897–4910 Preprint at <https://doi.org/10.1242/dev.02099> (2005).

54. Roux, M. & Zaffran, S. Hox genes in cardiovascular development and diseases. *Journal of Developmental Biology* vol. 4 Preprint at <https://doi.org/10.3390/jdb4020014> (2016).
55. Zhou, J. An emerging role for Hippo-YAP signaling in cardiovascular development. *Journal of Biomedical Research* vol. 28 251–254 Preprint at <https://doi.org/10.7555/JBR.28.20140020> (2014).
56. Xiao, Y., Leach, J., Wang, J. & Martin, J. F. Hippo/Yap Signaling in Cardiac Development and Regeneration. *Current Treatment Options in Cardiovascular Medicine* vol. 18 Preprint at <https://doi.org/10.1007/s11936-016-0461-y> (2016).
57. Lescroart, F. & Zaffran, S. Hox and tale transcription factors in heart development and disease. *International Journal of Developmental Biology* **62**, 837–846 (2018).
58. Bartlett, H., Veenstra, G. J. C. & Weeks, D. L. Examining the cardiac NK-2 genes in early heart development. in *Pediatric Cardiology* vol. 31 335–341 (2010).
59. Clark, C. D. *et al.* Evolutionary conservation of Nkx2.5 autoregulation in the second heart field. *Dev Biol* **374**, 198–209 (2013).
60. Akazawa, H. & Komuro, I. Cardiac transcription factor Csx/Nkx2-5: Its role in cardiac development and diseases. *Pharmacology and Therapeutics* vol. 107 252–268 Preprint at <https://doi.org/10.1016/j.pharmthera.2005.03.005> (2005).
61. Castelán-Muñoz, N. *et al.* MADS-box genes are key components of genetic regulatory networks involved in abiotic stress and plastic developmental responses in plants. *Frontiers in Plant Science* vol. 10 Preprint at <https://doi.org/10.3389/fpls.2019.00853> (2019).
62. Mokalled, M. H. *et al.* Myocardin-related transcription factors are required for cardiac development and function. *Dev Biol* **406**, 109–116 (2015).
63. Materna, S. C., Sinha, T., Barnes, R. M., Lammerts van Bueren, K. & Black, B. L. Cardiovascular development and survival require Mef2c function in the myocardial but not the endothelial lineage. *Dev Biol* **445**, 170–177 (2019).

64. Lockhart, M. M. *et al.* Mef2c Regulates Transcription of the Extracellular Matrix Protein Cartilage Link Protein 1 in the Developing Murine Heart. *PLoS One* **8**, (2013).
65. Dodou, E., Verzi, M. P., Anderson, J. P., Xu, S. M. & Black, B. L. Mef2c is a direct transcriptional target of ISL1 and GATA factors in the anterior heart field during mouse embryonic development. *Development* **131**, 3931–3942 (2004).
66. Qiao, X. H. *et al.* MEF2c loss-of-function mutation contributes to congenital heart defects. *Int J Med Sci* **14**, 1143–1153 (2017).
67. Franco, H. L., Casasnovas, J., Rodríguez-Medina, J. R. & Cadilla, C. L. Redundant or separate entities? - Roles of Twist1 and Twist2 as molecular switches during gene transcription. *Nucleic Acids Res* **39**, 1177–1186 (2011).
68. Vincentz, J. W., Barnes, R. M. & Firulli, A. B. Hand factors as regulators of cardiac morphogenesis and implications for congenital heart defects. *Birth Defects Research Part A - Clinical and Molecular Teratology* vol. 91 485–494 Preprint at <https://doi.org/10.1002/bdra.20796> (2011).
69. Lee, M. P. & Yutzey, K. E. Twist1 directly regulates genes that promote cell proliferation and migration in developing heart valves. *PLoS One* **6**, (2011).
70. Shelton, E. L. & Yutzey, K. E. Twist1 function in endocardial cushion cell proliferation, migration, and differentiation during heart valve development. *Dev Biol* **317**, 282–295 (2008).
71. Whitcomb, J., Gharibeh, L. & Nemer, M. From embryogenesis to adulthood: Critical role for GATA factors in heart development and function. *IUBMB Life* vol. 72 53–67 Preprint at <https://doi.org/10.1002/iub.2163> (2020).
72. Brewer, A. & Pizzey, J. GATA factors in vertebrate heart development and disease. *Expert Reviews in Molecular Medicine* vol. 8 1–20 Preprint at <https://doi.org/10.1017/S1462399406000093> (2006).
73. Wilson, V. & Conlon, F. L. *The T-box family*. <http://genomebiology.com/2002/3/6/reviews/3008.1>.

74. Plageman, T. F. & Yutzey, K. E. T-box genes and heart development: Putting the ‘T’ in heart. *Developmental Dynamics* **232**, 11–20 (2005).
75. Stirnimann, C. U., Ptchelkine, D., Grimm, C. & Müller, C. W. Structural Basis of TBX5 – DNA Recognition : The T-Box Domain in Its DNA-Bound and - Unbound Form. 71–81 (2010) doi:10.1016/j.jmb.2010.04.052.
76. The Role of Tbx20 in Cardiovascular Development and Function.
77. Liu, P., Sun, Y., Qiu, G., Jiang, H. & Qiu, G. Silencing of TBX20 gene expression in rat myocardial and human embryonic kidney cells leads to cell cycle arrest in G2 phase. *Mol Med Rep* **14**, 2904–2914 (2016).
78. Najand, N., Ryu, J. R. & Brook, W. J. In Vitro Site Selection of a Consensus Binding Site for the *Drosophila melanogaster* Tbx20 Homolog Midline. *PLoS One* **7**, (2012).
79. Kanamori, H. *et al.* The role of autophagy emerging in postinfarction cardiac remodelling. 330–339 (2018) doi:10.1093/cvr/cvr073.
80. Chakraborty, S., Sengupta, A. & Yutzey, K. E. Tbx20 promotes cardiomyocyte proliferation and persistence of fetal characteristics in adult mouse hearts. *J Mol Cell Cardiol* **62**, 203–213 (2013).
81. Bui, A. L., Horwich, T. B. & Fonarow, G. C. Epidemiology and risk profile of heart failure. *Nat Rev Cardiol* **8**, 30–41 (2011).
82. Prabhakaran, D. *et al.* Cardiovascular Diseases in India Compared With the United States. *J Am Coll Cardiol* **72**, 79–95 (2018).
83. Rodius, S. *et al.* Fisetin protects against cardiac cell death through reduction of ROS production and caspases activity. *Sci Rep* **10**, (2020).
84. Sakabe, N. J. *et al.* Dual transcriptional activator and repressor roles of TBX20 regulate adult cardiac structure and function. *Hum Mol Genet* **21**, 2194–2204 (2012).
85. Shen, T. *et al.* Tbx20 functions as an important regulator of estrogen-mediated cardiomyocyte protection during oxidative stress. *Int J Cardiol* **168**, 3704–3714 (2013).

86. Xiang, F. L., Guo, M. & Yutzey, K. E. Overexpression of Tbx20 in adult cardiomyocytes promotes proliferation and improves cardiac function after myocardial infarction. *Circulation* **133**, 1081–1092 (2016).
87. Lockhart, M., Wirrig, E., Phelps, A. & Wessels, A. Extracellular matrix and heart development. *Birth Defects Research Part A - Clinical and Molecular Teratology* vol. 91 535–550 Preprint at <https://doi.org/10.1002/bdra.20810> (2011).
88. Koch, C. D., Lee, C. M. & Apte, S. S. Aggrecan in Cardiovascular Development and Disease. *Journal of Histochemistry and Cytochemistry* vol. 68 777–795 Preprint at <https://doi.org/10.1369/0022155420952902> (2020).
89. Song, R. & Zhang, L. Cardiac ECM: Its epigenetic regulation and role in heart development and repair. *International Journal of Molecular Sciences* vol. 21 1–20 Preprint at <https://doi.org/10.3390/ijms21228610> (2020).
90. Frangogiannis, N. G. The extracellular matrix in myocardial injury , repair , and remodeling. **127**, (2017).
91. Newby, A. C. Dual role of matrix metalloproteinases (matrixins) in intimal thickening and atherosclerotic plaque rupture. *Physiol Rev* **85**, 1–31 (2005).
92. Manhenke, C. *et al.* The relationship between markers of extracellular cardiac matrix turnover : infarct healing and left ventricular remodelling following primary PCI in patients with first-time STEMI. 395–402 (2018) doi:10.1093/eurheartj/eh482.
93. Frangogiannis, N. G. The extracellular matrix in ischemic and nonischemic heart failure. *Circ Res* **125**, 117–146 (2019).
94. Pauschinger, M., Chandrasekharan, K. & Schultheiss, H.-P. *Myocardial Remodeling in Viral Heart Disease: Possible Interactions Between Inflammatory Mediators and MMP-TIMP System.* *Heart Failure Reviews* vol. 9 (2004).
95. Wang, F. & Muller, S. Manipulating autophagic processes in autoimmune diseases: A special focus on modulating chaperone-mediated autophagy, an emerging therapeutic target. *Front Immunol* **6**, 1–14 (2015).

96. Yang, J., Carra, S., Zhu, W. G. & Kampinga, H. H. The regulation of the autophagic network and its implications for human disease. *Int J Biol Sci* **9**, 1121–1133 (2013).
97. Srivastava, A. & Mohanty, S. K. Age and Sex Pattern of Cardiovascular Mortality, Hospitalisation and Associated Cost in India. *PLoS One* **8**, 1–13 (2013).
98. *8179 AGING*. www.aging-us.com (2022).
99. Chen, Y. *et al.* The Role of Tbx20 in Cardiovascular Development and Function. *Frontiers in Cell and Developmental Biology* vol. 9 Preprint at <https://doi.org/10.3389/fcell.2021.638542> (2021).
100. Chakraborty, S., Sengupta, A. & Yutzey, K. E. Journal of Molecular and Cellular Cardiology Tbx20 promotes cardiomyocyte proliferation and persistence of fetal characteristics in adult mouse hearts. *J Mol Cell Cardiol* **62**, 203–213 (2013).
101. Shen, T. *et al.* Tbx20 functions as an important regulator of estrogen-mediated cardiomyocyte protection during oxidative stress. *Int J Cardiol* **168**, 3704–3714 (2017).
102. Stennard, F. A. *et al.* Cardiac T-box factor Tbx20 directly interacts with Nkx2-5, GATA4, and GATA5 in regulation of gene expression in the developing heart. *Dev Biol* **262**, 206–224 (2003).
103. Kanamori, H. *et al.* Functional significance and morphological characterization of starvation-induced autophagy in the adult heart. *American Journal of Pathology* **174**, 1705–1714 (2009).
104. Mizushima, N., Yamamoto, A., Matsui, M., Yoshimori, T. & Ohsumi, Y. In Vivo Analysis of Autophagy in Response to Nutrient Starvation Using Transgenic Mice Expressing a Fluorescent Autophagosome Marker. *Mol Biol Cell* **15**, 1101–1111 (2004).
105. Khanam, R., Sengupta, A., Mukhopadhyay, D. & Chakraborty, S. Identification of Adamts4 as a novel adult cardiac injury biomarker with therapeutic implications in patients with cardiac injuries. *Sci Rep* **12**, (2022).

106. Chang, L. *et al.* MiR-181b-5p suppresses starvation-induced cardiomyocyte autophagy by targeting Hspa5. *Int J Mol Med* **43**, 143–154 (2019).
107. Evans-Anderson, H. J., Alfieri, C. M. & Yutzey, K. E. Regulation of cardiomyocyte proliferation and myocardial growth during development by FOXO transcription factors. *Circ Res* **102**, 686–694 (2008).
108. Polley, A., Khanam, R., Sengupta, A. & Chakraborty, S. Asporin Reduces Adult Aortic Valve Interstitial Cell Mineralization Induced by Osteogenic Media and Wnt Signaling Manipulation In Vitro. **2020**, (2020).
109. Khing, T. M. *et al.* The effect of paclitaxel on apoptosis, autophagy and mitotic catastrophe in AGS cells. *Sci Rep* **11**, (2021).
110. Sayers, E. W. *et al.* Database resources of the National Center for Biotechnology Information. *Nucleic Acids Res* **50**, D20 (2022).
111. Xiang, F. L., Guo, M. & Yutzey, K. E. Overexpression of Tbx20 in adult cardiomyocytes promotes proliferation and improves cardiac function after myocardial infarction. *Circulation* **133**, 1081–1092 (2016).
112. Stirnimann, C. U., Ptchelkine, D., Grimm, C. & Müller, C. W. Structural Basis of TBX5–DNA Recognition: The T-Box Domain in Its DNA-Bound and -Unbound Form. *J Mol Biol* **400**, 71–81 (2010).
113. Najand, N., Ryu, J. R. & Brook, W. J. In Vitro Site Selection of a Consensus Binding Site for the *Drosophila melanogaster* Tbx20 Homolog Midline. *PLoS One* **7**, (2012).
114. Zhou, J. *et al.* Loss of adult cardiac myocyte GSK-3 leads to mitotic catastrophe resulting in fatal dilated cardiomyopathy. *Circ Res* **118**, 1208–1222 (2016).
115. Chen, Y. *et al.* Ser9 phosphorylation of GSK-3 β promotes aging in the heart through suppression of autophagy. *The Journal of Cardiovascular Aging* (2021) doi:10.20517/jca.2021.13.
116. Rabinovich-Nikitin, I. & Kirshenbaum, L. A. GSK-3 β mediates cardiac senescence through inhibition of ULK1 directed autophagy. *The Journal of Cardiovascular Aging* (2021) doi:10.20517/jca.2021.24.

117. López-Muneta, L. *et al.* Generation of NKX2.5GFP Reporter Human iPSCs and Differentiation Into Functional Cardiac Fibroblasts. *Front Cell Dev Biol* **9**, (2022).
118. Bai, C. *et al.* Identification and biological characterization of chicken embryonic cardiac progenitor cells. *Cell Prolif* **46**, 232–242 (2013).
119. Sedlackova, L. & Korolchuk, V. I. The crosstalk of NAD, ROS and autophagy in cellular health and ageing. *Biogerontology* vol. 21 381–397 Preprint at <https://doi.org/10.1007/s10522-020-09864-0> (2020).
120. Fang, E. F. *et al.* NAD⁺ in Aging: Molecular Mechanisms and Translational Implications. *Trends in Molecular Medicine* vol. 23 899–916 Preprint at <https://doi.org/10.1016/j.molmed.2017.08.001> (2017).
121. Macindoe, I. *et al.* Conformational Stability and DNA Binding Specificity of the Cardiac T-Box Transcription Factor Tbx20. *J Mol Biol* **389**, 606–618 (2009).
122. Stennard, F. A. *et al.* Murine T-box transcription factor Tbx20 acts as a repressor during heart development , and is essential for adult heart integrity , function and adaptation. 2451–2462 (2010) doi:10.1242/dev.01799.
123. aging-v8i2-100881.
124. Yamamoto-Imoto, H. *et al.* Age-associated decline of MondoA drives cellular senescence through impaired autophagy and mitochondrial homeostasis. *Cell Rep* **38**, (2022).
125. Ryu, H. Y. *et al.* GSK3B induces autophagy by phosphorylating ULK1. *Exp Mol Med* **53**, 369–383 (2021).
126. Jin, J., Wang, G.-L., Shi, X., Darlington, G. J. & Timchenko, N. A. The Age-Associated Decline of Glycogen Synthase Kinase 3 β Plays a Critical Role in the Inhibition of Liver Regeneration. *Mol Cell Biol* **29**, 3867–3880 (2009).
127. Koike, R., Takaichi, Y., Soeda, Y. & Takashima, A. Memory formation in old age requires GSK-3 β . *Aging Brain* **1**, 100022 (2021).

128. Chen, Y. *et al.* Ser9 phosphorylation of GSK-3 β promotes aging in the heart through suppression of autophagy. *The Journal of Cardiovascular Aging* (2021) doi:10.20517/jca.2021.13.
129. Serpooshan, V. *et al.* Nkx2.5+ Cardiomyoblasts Contribute to Cardiomyogenesis in the Neonatal Heart. *Sci Rep* **7**, (2017).
130. Chen, C., Zhou, M., Ge, Y. & Wang, X. SIRT1 and aging related signaling pathways. *Mechanisms of Ageing and Development* vol. 187 Preprint at <https://doi.org/10.1016/j.mad.2020.111215> (2020).
131. aging-v8i2-100881.
132. Law, B., Fowlkes, V., Goldsmith, J. G., Carver, W. & Goldsmith, E. C. Diabetes-induced alterations in the extracellular matrix and their impact on myocardial function. in *Microscopy and Microanalysis* vol. 18 22–34 (2012).
133. Glasson, S. S. *et al.* Characterization of and osteoarthritis susceptibility in ADAMTS-4-knockout mice. *Arthritis Rheum* **50**, 2547–2558 (2004).
134. Johnston, L., Harding, S. A. & La Flamme, A. C. Comparing methods for ex vivo characterization of human monocyte phenotypes and in vitro responses. *Immunobiology* **220**, 1305–1310 (2015).
135. Fernández-Rojas, B., Vázquez-Cervantes, G. I., Pedraza-Chaverri, J. & Gutiérrez-Venegas, G. Lipoteichoic acid reduces antioxidant enzymes in H9c2 cells. *Toxicol Rep* **7**, 101–108 (2020).
136. Sengupta, A., Molkentin, J. D., Paik, J. H., DePinho, R. A. & Yutzey, K. E. FoxO transcription factors promote cardiomyocyte survival upon induction of oxidative stress. *Journal of Biological Chemistry* **286**, 7468–7478 (2011).
137. Ma, Y. *et al.* DPP-4 inhibitor anagliptin protects against hypoxia-induced cytotoxicity in cardiac H9C2 cells. *Artif Cells Nanomed Biotechnol* **47**, 3823–3831 (2019).
138. Sahadevan, P. & Allen, B. G. Isolation and culture of adult murine cardiac atrial and ventricular fibroblasts and myofibroblasts. *Methods* (2021) doi:10.1016/j.ymeth.2021.04.004.

139. Li, D., Wu, J., Bai, Y., Zhao, X. & Liu, L. Isolation and culture of adult mouse cardiomyocytes for cell signaling and in vitro cardiac hypertrophy. *Journal of Visualized Experiments* 2–9 (2014) doi:10.3791/51357.
140. Vukovic, V. *et al.* Hypoxia-inducible factor-1 α is an intrinsic marker for hypoxia in cervical cancer xenografts. *Cancer Res* **61**, 7394–7398 (2001).
141. Gao, Y., Chu, M., Hong, J., Shang, J. & Xu, D. Hypoxia induces cardiac fibroblast proliferation and phenotypic switch: A role for caveolae and caveolin-1/PTEN mediated pathway. *J Thorac Dis* **6**, 1458–1468 (2014).
142. Lijnen, P. J., van Pelt, J. F. & Fagard, R. H. Stimulation of reactive oxygen species and collagen synthesis by angiotensin II in cardiac fibroblasts. *Cardiovasc Ther* **30**, 1–8 (2012).
143. Walker, J. L., Bleaken, B. M., Romisher, A. R., Alnwibit, A. A. & Menko, A. S. In wound repair vimentin mediates the transition of mesenchymal leader cells to a myofibroblast phenotype. *Mol Biol Cell* **29**, 1555–1570 (2018).
144. Rog-Zielinska, E. A., Norris, R. A., Kohl, P. & Markwald, R. The Living scar - cardiac fibroblasts and the injured heart. *Trends Mol Med* **22**, 99–114 (2016).
145. Karsdal, M. A. *et al.* Collagen biology and non-invasive biomarkers of liver fibrosis. *Liver International* **40**, 736–750 (2020).
146. Hinderer, S. & Schenke-Layland, K. Cardiac fibrosis – A short review of causes and therapeutic strategies. *Adv Drug Deliv Rev* **146**, 77–82 (2019).
147. Rienks, M., Papageorgiou, A. P., Frangogiannis, N. G. & Heymans, S. Myocardial extracellular matrix: An ever-changing and diverse entity. *Circ Res* **114**, 872–888 (2014).
148. Miner, E. C. & Miller, W. L. A look between the cardiomyocytes: The extracellular matrix in heart failure. *Mayo Clin Proc* **81**, 71–76 (2006).
149. Frangogiannis, N. G. Cardiac fibrosis: Cell biological mechanisms, molecular pathways and therapeutic opportunities. *Mol Aspects Med* **65**, 70–99 (2019).
150. Rienks, M., Barallobre-Barreiro, J. & Mayr, M. The emerging role of the ADAMTS family in vascular diseases. *Circ Res* **123**, 1279–1281 (2018).

151. Perrucci, G. L., Rurali, E. & Pompilio, G. Cardiac fibrosis in regenerative medicine: Destroy to rebuild. *J Thorac Dis* **10**, S2376–S2389 (2018).
152. Kapelko, V. I. Extracellular matrix alterations in cardiomyopathy: The possible crucial role in the dilative form. *Exp Clin Cardiol* **6**, 41–49 (2001).
153. Chen, Y. *et al.* Association of Cardiovascular Disease with Premature Mortality in the United States. *JAMA Cardiol* **4**, 1230–1238 (2019).
154. Ordunez, P., Prieto-Lara, E., Gawryszewski, V. P., Hennis, A. J. M. & Cooper, R. S. Premature mortality from cardiovascular disease in the Americas - Will the goal of a decline of ‘25% by 2025’ be met? *PLoS One* **10**, (2015).
155. Obas, V. & Vasan, R. S. The aging heart. *Clinical Science* vol. 132 1367–1382 Preprint at <https://doi.org/10.1042/CS20171156> (2018).
156. Yan, M. *et al.* Cardiac Aging: From Basic Research to Therapeutics. *Oxidative Medicine and Cellular Longevity* vol. 2021 Preprint at <https://doi.org/10.1155/2021/9570325> (2021).
157. Das, S. *et al.* ER stress induces upregulation of transcription factor Tbx20 and downstream Bmp2 signaling to promote cardiomyocyte survival. *Journal of Biological Chemistry* **299**, 103031 (2023).
158. Olejarz, W., Łacheta, D. & Kubiak-Tomaszewska, G. Matrix metalloproteinases as biomarkers of atherosclerotic plaque instability. *International Journal of Molecular Sciences* vol. 21 Preprint at <https://doi.org/10.3390/ijms21113946> (2020).
159. Feldman, K. S., Pavlou, M. P. & Zahid, M. Cardiac Targeting Peptide : From Identification to Validation to Mechanism of Transduction. in *Methods in Molecular Biology* vol. 2211 97–112 (Humana Press Inc., 2021).
160. Kim, H. *et al.* Cardiac-specific delivery by cardiac tissue-targeting peptide-expressing exosomes. *Biochem Biophys Res Commun* **499**, 803–808 (2018).

Annexure

Annexure-I
List of reagents used

	Name of reagent	Catologue No.
1	Trizol	Ambion, 15596026
2	Chloroform	Merck, 1.94506.0521
3	Isopropanol	SRL (62986)
4	Molecular grade ethanol	Himedia,
5	DEPC (Diethyl pyrocarbonate)	Himedia, 46791
6	DNA Taq Polymerase Kit (Reverse Transcriptase PCR) A. Buffer B. dH ₂ O C. Taq Polymerase	1. Bioline, BIO-21040 2. Takara
7	TAE Buffer (50X-Stock, 1X-Working) 1. Tris Base 2. Glacial acetic acid	1. SRL, 71033

	<p>3. 0.5M EDTA</p> <p>4. dH₂O</p>	<p>2. SRL, 85801</p> <p>3. SRL, 43272</p>
8	<p>PBS (Phosphate Buffer Saline)</p> <p>1. Sodium Chloride (NaCl)</p> <p>2. Potassium Chloride (KCl)</p> <p>3. Di-Sodium hydrogen phosphate anhydrous (Na₂HPO₄)</p> <p>4. Potassium dihydrogen phosphate (KH₂HPO₄)</p>	
8	DNA Ladder (100bp)	<p>1. Bioline, 33030</p> <p>2. Bio-Rad, 1708202</p> <p>3. Promega, G2101</p>
9	Gel loading buffer	<p>1. Bio-Rad, 1610737</p> <p>2. Invitrogen</p> <p>3. Promega</p>
10	Ethidium Bromide	<p>1. SRL, 17220</p> <p>2. Promega</p>
11	<p>Real Time PCR Kit (SYBR Green Supermix)</p> <p>A. dH₂O</p>	Bio-Rad, 170-8885

	B. SYBR Green Mix	
12	<p>PBS (Phosphate Buffer Saline) pH-7.4</p> <ol style="list-style-type: none"> 1. Sodium Chloride (NaCl) 2. Potassium Chloride (KCl) 3. Di-Sodium hydrogen phosphate anhydrous (Na₂HPO₄) 4. Potassium dihydrogen phosphate (KH₂HPO₄) 	<ol style="list-style-type: none"> 1. SRL, 33204 2. SRL, 84984 3. SRL, 21669 4. Merck, 7778-77-0
13.	DMEM nutrient Media	Himedia, AT1007
14	DMEM nutrient media	Himedia, AT195
15	<p>Collagen Solution</p> <ol style="list-style-type: none"> 1. dH₂O 2. 10X PBS 3. 1N NaOH 4. Rat tail collagen (3mg/ml) 	<ol style="list-style-type: none"> 3. SRL-68151 4. Gibco, A10483-01
16	Fetal Bovine Serum	Himedia, RM10409

17	Penicillin- Streptomycin	1. Invitrogen, 15140122 2. Himedia, A004
18	Paraformaldehyde	1. Affymetrix, 19943 2. Himedia
19	TritonX-100	SRL, 64518
20	Histopaque	Sigma, 1077
21	Np40 solution 1. Tris HCl (50mM) 2. NaCl (150mM) 3. BSA (5mg/ml) 4. NP40 [IGEPAL, NP40 supplement] (0.5%)	1. SRL, 89781 2. Merck (106404) 3. SRL, 14438 4. Sigma, 198596
22	Rapamycin	Himedia, TC416-10mg
23	Trypsin -EDTA	Himedia, TCL007-100ml
24	gentamycin amphotericin B soln 1000X	Himedia, A031-20ml
25	0.2 um syringe filter	Himedia, SF143-50No
26	Tris Buffer base	SRL, 71033
27	Tween20	Promega, H5152

28	Glycine	SRL, 66327
29	BSA	SRL, 85171
30	HEPES (molecular grade)	Promega, H5302
31	APS	SRL, 65553
32	TEMED	SRL, 52145
33	Acrylamide/Bisacrylamide	SRL, 38862
34	SDS	Himedia, GRM205-100G
35	Collagenase- type II	1. Sigma, 234153 2. Gibco, 17101-015
36	Protease Inhibitor	1. Roche, 11429868 2. Genetix GX-2811AR
37	Phosphatase Inhibitor	Genetix, GX-0211AR
38	Glycerol	Merck, 104057
39	N-propyl gallate	Sigma, P3130
40	Mounting media 1. 90% glycerol	

	2. 0.5% N-propyl gallate 3. 20mM Tris (pH- 8)	
41	Bradford's Reagent	BioRad, 500-006
42	Lipofectamine-RNAiMAX	Invitrogen, 13778-075
43	Adamts4 siRNA	Ambion, 4390771
44	Tbx20 siRNA	Ambion, 4390771
45	Scrambled siRNA	Ambion, 4390843
46	SB431542	Abcam, ab120163
47	Anaerogas pack	Himedia, LE200A
48	H ₂ O ₂	Merck, 107209
49	cDNA synthesis kit	BioRad, 170-884
50	Primers (enlisted in Annexure-II)	IDT
51	Cholesterol reagent	Erba, 120194
52	Triglyceride kit	Erba, 121175
53	DMSO	Life technologies, D12345

<p>54</p>	<p>Primary antibodies</p> <ol style="list-style-type: none"> 1. Tbx20 2. Lc3b 3. Beclin-1 4. Nkx2.5 5. Gata4 6. GSK-3β 7. pGSK-3β 8. Sirtuin-1 9. Adamts4 10. Tgf-β1 11. Collagen-III 12. α-SMA 13. Periostin 14. Vimentin 15. MF20 	<ol style="list-style-type: none"> 1. Invitrogen, PA5-40669 2. Abcam, b48394 3. Abcam, ab207612 4. Invitrogen, PA5-85215 5. Abcam, ab227512 6. CST, 27C10 7. Abcam, ab131097 8. Genetex, GTX134606 9. Invitrogen, PA1-1749A 10. Abcam, ab64715 11. Abcam, ab 7778 12. Invitrogen, 14-976082 13. Abcam, ab14041 14. Abcam, ab17321 15. DHSB, AB2147781
<p>55</p>	<p>Secondary antibodies</p> <ol style="list-style-type: none"> 1. Rabbit polyclonal 2. Mouse polyclonal 3. Mouse polyclonal^{HRP} 4. Rabbit polyclonal^{HRP} 	<ol style="list-style-type: none"> 1. Alexafluor 488, Abcam, ab150077 2. Alexafluor 594, Abcam, ab150116, Alexafluor 488, Abcam,

		<p>3. Abcam, ab97023</p> <p>4. Abcam, ab97051</p>
56	Apotosis/ Necrosis assay kit	Abcam, ab176749
57	<p>Mammalian cell lysis buffer</p> <p>1. Tris HCl (pH-8), 50mM</p> <p>2. NaCl (150mM)</p> <p>3. 0.1% Triton-X-100</p> <p>4. 0.5% Sodium Deoxycholate</p> <p>5. 0.1% Sodium dodecyl sulphate (SDS)</p> <p>6. Sodium Orthovanadate (1mM)</p> <p>7. Sodium fluoride, NaF (1mM)</p>	<p>1. SRL, 71033</p> <p>2. Merck (106404)</p> <p>3. SRL, 64518</p> <p>4. SRL, 96876</p> <p>5. Himedia, GRM205</p> <p>6. SRL, 86766</p> <p>7. SRL, 29821</p>
58	<p>Myocyte Perfusion Buffer (pH-7.4)</p> <p>1. NaCl</p> <p>2. KCl</p> <p>3. KH₂PO₄</p> <p>4. MgSO₄.7H₂O</p> <p>5. Na-HEPES</p> <p>6. NaHCO₃</p> <p>7. Taurine</p> <p>8. BDM</p> <p>9. Dextrose</p>	<p>6. SRL, 144-55-8</p> <p>7. Sigma, T0625</p> <p>8. Sigma, B0753</p> <p>9. Merck, 108337</p>
59	Myocyte Digestion Buffer	

	<ol style="list-style-type: none"> 1. 100mM CaCl₂ 2. Collagenase -II 	1. Merck, 102391
60	<p>Myocyte Stopping Buffer</p> <ol style="list-style-type: none"> 1. Perfusion buffer 2. FBS 3. 10mM CaCl₂ 	
61	<p>Dissociation medium</p> <ol style="list-style-type: none"> 1. NaCl 2. Hepes 3. NaH₂PO₄ 4. KCl 5. Dextrose 6. MgSO₄ 7. BSA 8. CaCl₂, 1.0 M 9. Collagenase-Type II 10. Pancreatin 11. Milli-Q water 	10. SRL, 41421
62	DAPI	Sigma, D9542
63	Phalloidin	CST, 8878S
64	Coomasie Brillaint blue	SRL, 84778

65	2X Laemmli Buffer	BioRad, 610737
66	Running Buffer (Tris/Glycine/SDS) 1. Tris (25mM) 2. Glycine(190mM) 3. 0.1%SDS	
67	Transfer Buffer 1. Tris (25mM) 2. Glycine(190mM) 3. 20%Methanol	3. SRL. 65524
68	Tris-buffered saline with Tween20 (TBST) solution 1. Tris, pH=7.5 (20mM) 2. NaCl(150mM) 3. 0.1 % Tween20	
69	Blocking Buffer 1. Non-fat dry milk (5%) 2. TBST	
70	Antibody solvent	

	<ol style="list-style-type: none"> 1. BSA (5%) 2. TBST 	
71	Western ECL Substrate	BioRad, 1705060
72	Coomassie Stain <ol style="list-style-type: none"> 1. Coomassie Brillaint blue 2. Acetic acid 3. Methanol 	
73	Coomassie de-staining solution <ol style="list-style-type: none"> 1. Methanol 2. Acetic acid 3. dH₂O 	
74	Citrate buffer (pH-6) <ol style="list-style-type: none"> 1. 10mM Na-Citrate 2. Tween 20 3. dH₂O 	1. SRL, 67331
75	Adamts4 ELISA kit	Abcam, ab213753
76	Poly-l-lysine	Sigma, P8920
77	Paraffin	Merck, V800291
78	Xylene	Merck, 534056

Annexure-II
List of Primers

Gene name	Annealing temperature (°C)	Amplification size (bp)	Primer sequence
Rat			
<i>β-actin</i>	55	189	F: 5'-TCTTCCAGCCCTTCCTTCCTG-3' R: 5'-CACACAGAGTACTTGCGCTC-3'
<i>Adamts4</i>	60	163	F: 5'-TCATGAACTGGGCCATGTCT-3' R: 5'-TTCCTGCTCTGTCTGGTGAG-3'
<i>Hif-1α</i>	58.8	218	F: 5'-CCAGCAGACCCAGTTACAGA-3' R: 5'-TTCCTGCTCTGTCTGGTGAG-3'
<i>Catalase</i>	59.2	173	F: 5'-CCTCGTTCAGGATGTGGTTT-3' R: 5'-TCTGGTGATATCGTGGGTGA-3'
<i>Glut1</i>	55	320	F: 5'-AGAGGTCAAAGCAGAAA-3' R: 5'-CACCAGAAAGAAGATGAAG-3'
<i>Col-III</i>	53.2	131	F: 5'- CTGGTCCTGTTGGTCCATCT-3' R: 5'- ACCTTTGTACCTCGTGGAC-3'

<i>α-SMA</i>	58	188	F: 5'-CATCATGCGTCTGGACTTGG-3' R: 5'-CCAGGGAAGAAGAGGAAGCA-3'
<i>Beclin1</i>	60	200	F: 5'-AGTTTTTCAGAGCACAGCACG-3' R: 5'-TGTCCCTTCCCCACATTACC-3'
<i>mTORC1</i>	58.4	210	F: 5'-TCTGCACTTGTTGTTGCCTC-3' R: 5'-ACAATCGGGTGAATGATGCG-3'
<i>Lc3b</i>	58	234	F: 5'-CGTCCTGGACAAGACCAAGT-3' R: 5'-AGTGCTGTCCCGAACGTCTC-3'
Mouse			
<i>β-actin</i>	55	230	F: 5'-CCTCTATGCCAACACAGTGC-3' R: 5'-CCTGCTTGCTGATCCACATC-3'
<i>Tbx20</i>	58	167	F: 5'-CCCCGCTGCCAGCCAGGCTCTA-3' R: 5'-GTGCACCCGTGGCTGGTACTTATG C-3'
<i>Gabarapl1</i>	56.1	193	F: 5'-CATCGTGGAGAAGGCTCCTA-3' R: 5'-ATACAGCTGTCCCATGGTAG-3'
<i>Beclin1</i>	60	190	F: 5'-CAGGAGCTGGAAGATGTGGA-3' R: 5'-TTCGTCATCCAACCTCCAGCT-3'
<i>Tgf-β1</i>	55.4	249	F: 5'-CTGAACCAAGGAGACGGAATAC-3' R: 5'-CTCTGTGGAGCTGAAGCAATAG-3'
<i>Sirt1</i>	58	210	F: 5'-GGAACCTTTGCCTCATCTAC-3' R: 5'-CAGGTGAACTTGAGTCTTCC-3'

Annexure-III

Protocols

A. Rat myoblast cell line H9c2 cell culture

1. Stock H9C2 cell plates are obtained from Dr. Arun Bandopadhyay's lab (Indian Institute of Chemical Biology, IICB-Kolkata)
2. Cells are maintained in DMEM complete media (DMEM supplemented with FBS and Pen-Strep) at 37 °C in a humidified incubator with 95% air and 5% CO₂ levels maintained and maintained with regular passage.
3. Cells were seeded from stock plates according to the requirements for experimentation .

B. RNA isolation (from cells)

1. Cell media is aspirated from petridishes.
2. Cells are washed 2X PBS (3 ml for 100 mm dish and 1 ml for 60mm dish)
3. 500 µl of Trizol is added for 100mm plates and 200 µl of Trizol is added for 60mm plates and scrapped with a cell scrapper.
4. The trizol solution with dissociated cells are collected in microcentrifuge tubes to which 1/5th by volume chloroform is added and vortexed for 10 secs and kept chilled in ice for 1-2 minutes.
5. The microcentrifuge tubes with the samples are centrifuged at 12000g for 15 min at 4°C.
6. The upper aqueous layer is aspirated in another tube to which 1/2 volume (of Trizol) Isopropanol is added and incubated at -80°C for 1 hour, following which the samples are again centrifuged at 12000g for 10 min at 4°C.
7. The supernatant is decanted and to the almost invisible pellet, equal part by volume (of Trizol) of 75% ethanol (molecular grade) is added.

8. The cells are again centrifuged at 7500g for 5 min at 4°C.
9. The RNA pellets are air dried in laminar for a maximum of 5 mins.
10. RNA pellets are resuspended in nuclease free water (can also be placed in water bath at 60°C if the pellet obtained is a hard one, not easy to solubilise).
11. Concentration of RNA is measured and the samples are stored at -80°C until further usage.

C. RNA isolation (from tissue)

1. Dissection of adult heart from the diaphragm, heart bisected and collected in microcentrifuge tubes.
2. 500µl of Trizol to be added for 100mg of tissue.
3. The tissue samples are dissociated with the help of a homogeniser, after every 20 sec, a flash chill in ice for 45 sec until the tissue becomes homogenised in texture.
4. Steps 4-11 of the above protocol are followed.

D. RNA Spectrophotometry

1. Samples are diluted if necessary.
2. Samples are measured for concentration at 260nm and for purity assessment a ratio of absorbance at 260 and 280 nm are taken.
3. Absorbance is obtained on basis of Lambert Beer's law.

E. cDNA synthesis

1. Mini microcentrifuge tubes (200µl) are taken for cDNA synthesis
2. RNA equivalent to 1µg concentration is taken for cDNA synthesis.
3. First, dH₂O according to the volume of RNA, is added to the tube.

4. 4 μ l of cDNA supermix (Buffer+dNTPs+ reverse transcriptase) is added to the tube.
5. Required RNA is added to the tube.
6. Samples are given a short spin to ensure all the reagents are in solution.
7. The PCR tubes are placed in a thermal cycler for cDNA synthesis program.
8. The program is followed according to manufacturer's instructions:

Step1	Step2	Step3	Step4
25°C	46°C	95°C	4°C
5	30	1	∞

F. Primer design and standardisation

1. FASTA sequences obtained from NCBI website are submitted in the IDT primer designing tool portal.
2. Parameters such as T_m , secondary structures, GC content, enthalpy are considered before choosing the primer pair.
3. Primers generated are used for PCR and q-PCR assays.
4. Gradient PCR of annealing temperature is set according to T_m (e.g. 50°-60°C) of every primers
5. Best and most intense band intensity among the given number of samples is selected for further PCR and qPCR reactions separately.

G. Reverse Transcriptase PCR

1. In mini microcentrifuge / PCR tubes, the reactions for a total of 20 μ l volume are set according to the manufacturers protocol give below.

Reagent	Volume
dH ₂ O	15.6
Buffer	2
dNTP	0.4
Forward Primer	0.4
Reverse Primer	0.4
Taq polymerase	0.2
cDNA	1
Total volume	20 μ l

2. In a thermal cycler, the PCR tubes are placed for RT-PCR is reaction to take place as tabulated below.

Step1	Step2	Step3	Step4	Step5	Step6	Step7
94°C	94°C	Annealing Temperature	72°C	Go to Step2	72°C	4°C
3 mins	30 sec	40 secs	45 secs	35 cycles	5 mins	∞

H. Agarose gel electrophoresis:

Materials needed:

1. Electrophoresis chamber

2. Power Supply
3. Gel casting trays
4. Sample combs
5. Electrophoresis buffer
6. Loading buffer/dye
7. Ethidium bromide
8. Magnetic stirrer
9. Transilluminator

Recipe of TAE buffer

50X TAE Buffer composition

Reagent	Volume
Tris base	60.5g
Glacial acetic acid	14.27 ml
0.5 M EDTA (pH-8)	25 ml
dH ₂ O	Make up volume upto 250ml
Total	250 ml

Procedure:

1. 2% Agarose gel slabs are used for PCR products
2. Products are loaded for electrophoresis in 1X TAE running buffer
3. Gel loading dye (bromophenol blue) is mixed with PCR products to detect the migration.
4. 100bp DNA ladder is used to compare the product size of the unknown samples

5. After running, gels are imaged in transilluminator

I. Real time PCR (qPCR)

1. In a PCR tube, qPCR mix (SYBR mix) is set and distributed in 96 well hard shell PCR plates.
2. SYBR green super mix (Buffer+dNTPs+MgCl₂+ Taq polymerase) is used for each 10µl reaction.
3. Reaction set as according to the given protocol

Reagent	Volume (µl)
Primer 1	0.4
Primer 2	0.4
dH ₂ O	3.2
SYBR	5
cDNA	1
Total volume	10 µl

4. The 96 well plate with the reactions are placed in a qPCR thermal cycler and the reaction is performed with the help of BioRad CFX maestro software.
5. Results are obtained through the software at the end of run.

J. Phalloidin Staining:

1. Media is aspirated out from the cell plates
2. Washed twice in 1X PBS (1ml/60mm plate)
3. Cells are fixed in 4% paraformaldehyde (PFA) for 5 mins
4. Washed in 1X NP40 (500 µl/ chamber slide, 1ml/60mm plate) for 10 mins. (can be manipulated based on the condition of the cells]
5. Cells are kept in blocking for 1hr

6. Phalloidin stain is added (1:400 dilution) to the cell plates
7. Incubated for 1.5 hour
8. Cells are washed with 1X NP40 (1ml/60mm plate) [$\times 3$, 5mins each]
8. Add DAPI (1:400) and incubate in dark for 5 mins.
9. Washed with 1X PBS (x3, 5 mins each)
10. Cover slips mounted in mounting media.
11. Stored at 4°C.
12. Proceeded with microscopic imaging.

K. Antibody Staining:

1. Cell media are aspirated out from the plates.
2. Plates are rinsed with 1XPBS [$\times 2$]
3. Cells are fixed with 4% PFA (3mins)
4. Washed in TritonX-100 (10 mins).(This permeabilization step is omitted for staining with ECM markers).
5. Washed with 1X PBS (x3, 5mins each)
6. Blocking solution (3% BSA, 0.1% Triton-X100 in PBS) is added to the cells and incubated in an orbital shaker for 1 hour.
7. Cells are washed with 1X PBS.
8. Cells are incubated with overnight primary antibody (according to required dilution) incubation at 4°C.
9. Primary antibody is aspirated , cells are washed with 1X PBS (x3, 5 mins each) the following day and the cells are incubated in dark with secondary antibody (as per mentioned and required dilution) at room temperature for up to 2 hours.
10. Secondary antibody is aspirated and again cells are washed in 1X PBS (x3, 5mins each).
11. The nuclei are stained with DAPI (1:400) for 5 mins in dark.

12. Cells are washed in 1X PBS (x3, 5mins each).
13. Mounted in mounting media, cover slips are then stored at 4°C immediately.
14. Proceeded with imaging.

L. Immunohistochemistry (antibody staining with tissue sections)

1. Slides (5-6 micron sections) were dried in a 60°C hot air oven for an hour.
2. Deparaffinize in xylene (x3, 7 mins each).
3. Rehydrate slides in a series of graded ethanol: 100% (x2, 2 mins), then 2 mins each in 95%, 75% and 50% alcohol.
4. Wash in distilled water.
5. The slides are placed in coplin jars with antigen retrieval solution (citrate buffer) in a water bath for 25-30 mins at 90°C.
6. The coplin jar is taken out of the water bath and the solution is cooled to room temperature.
7. The slides are washed in 1X PBS (x2, 2 mins each).
8. Repeat steps 4-13 of the above mentioned antibody staining protocol.
9. Proceed for imaging under a microscope.

M. Tissue embedding and microtomy

1. The dissected heart tissue samples are fixed overnight in 4% PFA.
2. Washed with 1X PBS (x3, 5 mins) the following day.
3. Dehydrate tissue sample in a series of graded ethanol: 15 mins each in 50%, 70%, 80% 90% and (x2, 15 mins) in 100% alcohol.
4. Xylene added to dehydrated tissue samples for 5 mins.
5. In hot air oven, the xylene treated sample is added to a 1:1 xylene: paraffin solution for 30 mins at 60°C

6. Samples transferred to pure melt paraffin (x2, 40 mins each).
7. In a casting mould, melted wax is added to which sample from step 6 is added and any remaining air bubble is cleared with the help of hot scalpel.
8. The tissue embedded paraffin block is kept at 4°C until proceeding for sectioning (microtomy).
9. With the use of microtome (Leica microtome), the ribbon sections of 5 micron are cut and stretched out in a water bath set at 53-55°C and the stretched sections are collected on Poly-L- lysine precoated slides.
10. The slides are dried at 40°C for 30 mins in a hot air oven and stored in slide box at room temperature until further use.

N. Western Blot

Reagents to be prepared:

1. Cell lysis Lysis buffer.
2. Loading buffer (Laemmli buffer)
3. Running buffer (Tris/glycine/SDS)
4. Transfer buffer (Tris/glycine/Methanol)
5. Tris-buffered saline (TBS)
6. Tris-buffered saline with Tween20 (TBST) buffer
7. Blocking buffer

Procedure

Protein extraction from the cells and tissue samples

1. Cell media are aspirated out from the plates .
2. Cells are washed in ice cold 1X PBS.

3. Cells are scrapped with 2 ml of ice cold PBS (for 100 mm petridish) and centrifuged at 4000g for 15 mins at 4°C.
4. To the cell pellet, cell lysis buffer is added (varying from 100 – 200 μ l depending on the pellet).
5. Cells are vortexed for 10-15 secs twice after intermittent snap chill .
6. Protease and phosphatase inhibitors are added in the required ratio.
7. For tissue samples, lysis buffer (5-6 times by volume of the weight of tissue is added) with protease and phosphatase inhibitors added to it are homogenised.
8. The samples are centrifuged at 16000g for 20 mins at 4°C.
9. The supernatant is pipetted out and transferred into another tube.
10. The protein sample is stored as small aliquots at -20°C for short term use and at -80°C for long term storage.
11. Protein concentration is determined at 595nm against a known BSA standard using Bradford's reagent.

SDS PAGE electrophoresis

1. 10% SDS PAGE (or 7.5% or 12 %gel is cast depending on the size of the protein required) is prepared . proteins
2. An equal volume of protein (generally 70 μ g) and 2X Laemmli buffer is taken in microcentrifuge tubes and boiled for 5 mins at 95°C followed by snap chill.
3. Gel is run for 20mins at 40V
4. Voltage is increased up to 100-120V and run for 1-1.5hrs
5. The gel is stained with 10% Coomassie stain to check for whole protein and imaging is done with the help of a Chemi Doc. For WB, gels after run are proceeded for transfer to PVDF membranes.

Transferring the protein from gel to membrane

1. The gel is placed in 1X transfer buffer.
2. Transfer sandwich is assembled following the sequence (Mesh>filter paper>Gel>PVDF membrane>filter paper>mesh) . The blot is at the cathode and gel at the anode.
3. Transfer cassette is placed in a tank and kept at cold-room and run at 100V for 1 hour or at 10V overnight (if required).

Antibody incubation and imaging

1. Bot is rinsed with TBST solution
2. Blot is stripped / cut according to marker with molecular weight of protein required.
3. Then the blot is blocked in blocking solution (5% non-fat dry milk in TBST) for 1hr at RT .
4. The blot is washed in TBST (x2, 5 mins each)
5. Primary antibody is added to blots in 3% BSA solution.
6. Blots are incubated for overnight at 4°C
7. Next day, blots are washed with TBST solution (×2, 5mins each)
8. Blots are incubated with secondary HRP conjugated antibodies (added according to required dilution) for 2 hours at RT.
9. The blots are rinsed thrice with TBST for 5 mins each and proceeded with imaging in a ChemiDoc after adding a chemiluminescent reagent (BioRad ECl Clarity substrate).

Primary adult mice cardiac fibroblast culture

Cardiac fibroblasts isolation is adapted from the published protocol as mentioned below:

1. Excise the heart under sterile condition.
2. Remove the aorta
3. Separate the atria and ventricles
4. Mince tissue to ~1 mm size
5. Enzymatic digestion in dissociation medium (15 min, 37°C, gentle agitation).
6. Centrifuge tissue digest at 1500 rpm for 5 minutes and resuspended the pellets in 1 ml of DMEM medium.
7. Repeat steps 5-6 for another 10 rounds or until completely digested.
8. Pool pellets and centrifuge at 1500 rpm for 7 minutes.
9. Preplate cell pellet on Collagen coated Petri plates.
10. After 150 mins of pre-plating, media is aspirated to remove non-adherent cells and debris and fresh complete DMEM medium is added to it.
11. The cells are allowed to grow for a week with fresh media change given every day after which experiments are proceeded with.

Primary adult mice cardiomyocytes culture

Isolation of adult mouse cardiomyocytes is followed as described by Liu *et al.* as mentioned earlier in the methods section of Chapter 3 of this thesis except for the Langendorff perfusion set-up which was replaced by mechanical perfusion set-up. The cells were used for further experiments at about 75-80% confluency

Isolation of peripheral blood mononuclear cells (PBMCs)

1. To a 15 ml centrifuge tube, 3ml of Histopaque-1077 was added and brought to RT.
2. 3 ml of whole blood was transferred on top of histopaque layer and centrifuged at 400g for 30 mins at RT.
3. The upper layer was carefully aspirated with a Pasteur pipette without interfering the layer containing the mononuclear cells. The upper layer was discarded.
4. The opaque interface containing the mononuclear cells was transferred to a fresh centrifuge tube and washed with 10 ml of isotonic PBS by gently drawing in and out with a pipette tip.
5. Centrifuged at 250g for 10 mins at RT.
6. The supernatant was discarded and the cells were resuspended with 5ml of PBS.
7. Centrifuged again at 250g for 10 mins at RT.
8. Repeat step 6-7.
9. Resuspend the cells in PBS or culture media and plate for cell culture or add lysis buffer and proceed with WB.



OPEN

Identification of Adamts4 as a novel adult cardiac injury biomarker with therapeutic implications in patients with cardiac injuries

Riffat Khanam¹, Arunima Sengupta², Dipankar Mukhopadhyay³ & Santanu Chakraborty^{1✉}

Pathological cardiac remodeling as an aftermath of a severe cardiac injury can lead to ventricular dysfunction and subsequent heart failure. Adamts4, a metalloproteinase, and disintegrin with thrombospondin-like motif, involved in the turnover of certain extracellular matrix molecules and pathogenesis of osteoarthritis, also plays a role in cardiac remodeling although little is presently known about its expression and function in the heart. Here, we have investigated the dynamic expression pattern of Adamts4 during cardiogenesis and also in the adult heart. To our surprise, adult cardiac injury reactivated Adamts4 expression concomitant with fibrosis induction. To better understand the mechanism, cultured H9c2 cardiomyocyte cells were subjected to ROS injury and Hypoxia. Moreover, through combinatorial treatment with SB431542 (an inhibitor of Tgf- β 1), and Adamts4 siRNA mediated gene knockdown, we were able to decipher a regulatory hierarchy to the signal cascade being at the heart of Tgf- β regulation. Besides the hallmark expression of Adamts4 and Tgf- β 1, expression of other fibrosis-related markers like Collagen-III, alpha-SMA and Periostin were also assessed. Finally, increased levels of Adamts4 and alpha-SMA proteins in cardiac patients also resonated well with our animal and cell culture studies. Overall, in this study, we highlight, Adamts4 as a novel biomarker of adult cardiac injury.

Heart failure remains a global cause of mortality and morbidity and an issue of public health concern with over 20 million people diagnosed with at least first-time heart failure across the world^{1,2}. By 2016, at least 30 and 50 million cases of cardiovascular diseases (CVD) were recorded in the US and India respectively with a mortality rate of more than 70% in India³. Extracellular matrix (ECM) remodeling in heart is one of the contributing factors of pathogenesis in cardiovascular diseases^{4,5}. Collagen-I forms the major component of matrix interstitium of the myocardium, the other components of ECM include Collagen-III, fibronectin, proteoglycans, matrix metalloproteinases (MMPs), and tissue inhibitors of matrix metalloproteinases (TIMPs). The proportion and biochemistry of the ECM change due to underlying pressure overload, cardiac injury, myocardial infarction (MI), and/or ischemia-reperfusion (I/R) injury that leads to extracellular matrix reorganization which in turn is modulated by changes in turnover of matrix proteins⁶. A typical cardiac remodeling post-cardiac injury undergoes, three major phases namely inflammatory, proliferative and maturation leading to a mature scar formation⁷.

Although the initial stages of ECM remodeling are essential as it prevents rupture of the ventricular wall and prevents ventricular dilatation, however, extensive and unregulated ECM remodeling leads to progressive fibrosis in the heart and impairment of cardiac functioning^{8–10}.

The MMPs are a family of zinc-dependent proteases involved in the turnover of collagen¹¹. An important MMP is the Adamts family which apart from inhabiting the functions of an MMP also acts as disintegrins. Adamts4 a member of the Adamts family is a metalloproteinase and a disintegrin with thrombospondin like motifs^{10,12}. Adamts4 has been known to bind to the ECM proteins and executes cleavage of ECM proteoglycans like aggrecan, versican and brevican apart from regulating collagen turnover. There is not sufficient information in the context of cardiac remodeling with a focus on the involvement of Adamts4. So far it is known that Adamts4 knockout in animal models leads to a reduction in plaques in cases of high fat induced atherosclerosis¹³ and also, inhibition of Adamts4 with pentosan polysulfate following aortic banding improves cardiac functioning⁶.

¹Department of Life Sciences, Presidency University, Kolkata 700073, India. ²Department of Life Science and Biotechnology, Jadavpur University, Kolkata 700032, India. ³Department of Cardiology, Institute of Post Graduate Medical Education and Research (IPGME&R), SSKM Hospital, Kolkata 700020, India. ✉email: santanu.dbs@presiuniv.ac.in

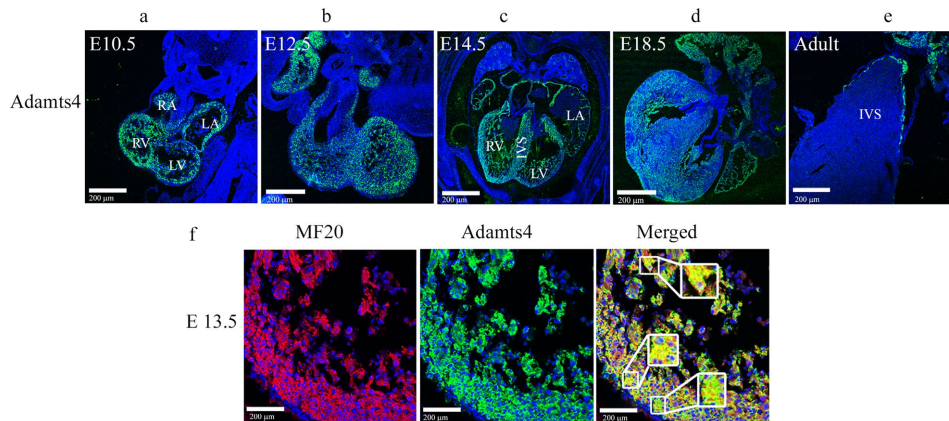


Figure 1. Dynamic expression of Adamts4 protein in embryonic and adult heart. Adamts4 expression is shown in developing E10.5 (a), E12.5 (b), E14.5 (c), E18.5 (d) adult (e) murine hearts. IHC with anti-Adamts4 antibody (green colour) and Topro3 (blue colour) used as nuclear stain, the expression pattern of Adamts4 is observed in (a)–(e). While the expression pattern of Adamts4 is more widespread in the embryonic stages throughout the RA, LA, RV, LV and IVS (a–d), the expression drastically reduces and is mainly only confined at the IVS in the adult stage (e) displaying a sharp contrast between the expression of Adamts4 in developing and adult stages. (f) Highlights the colocalization of Adamts4 (green) in the chamber myocardium with E13.5 chamber cardiomyocytes shows colocalization of Adamts4 with MF20 (shown in yellow colour) across the LV of chamber myocardium. The arrowheads point towards cells that have colocalized with both the markers i.e. Adamts4 and MF20. This confirms the expression of Adamts4 in embryonic cardiomyocytes. n = 4.

However, there is not much literature about Adamts4 expression and function in the developing and adult heart at the basal level and also in post cardiac injury. Only recently studies have shown that Adamts4 along with Adamts1 levels remain elevated in patients with acute aortic dissection and also in patients with coronary artery disease^{14,15}.

Here in our present study, for the first time, we aim to identify Adamts4 as a novel biomarker of adult cardiac injury under stress conditions. We have detected a strong expression of Adamts4 protein in the developing cardiac chamber myocardium in utero compared to very restricted expression in the adult murine hearts. To our surprise, we have also detected the expression of Adamts4 in vivo murine model of myocardial infarction (MI), localized in adult cardiomyocytes. To better understand the molecular insights of Adamts4 induction and associated affected signaling pathway activation, we have used H9c2, a rat ventricular myoblast cell line for several in vitro assays. Likewise, Adamts4 expression was induced in H9c2 cells, subjected to hypoxia (Hyp) and ROS injury inductions in vitro. Moreover, we manipulated the expression of Adamts4 with siRNA-mediated loss of function and TGF- β inhibitor studies in H9c2 cells to evaluate its regulation and dependency on TGF- β signaling since TGF- β has been long known to be a characteristic marker for inflammatory and fibrotic responses following pathological stress including MI, ischemia and reperfusion (I/R) injury^{16–20}. Finally and most importantly, we also validated our hypothesis in human clinical samples and demonstrated the induced expression of ADAMTS4 in patients with indicated cardiac ailments.

Results

Dynamic expression pattern of murine Adamts4 protein observed in developing and adult hearts. Immunohistochemistry (IHC) with anti-Adamts4 antibody shows Adamts4 protein expresses strongly in developing murine cardiac chambers but the expression significantly wanes in adult murine hearts. In contrast to the adult heart (Fig. 1e) where Adamts4 expression is largely restricted at the edge of the interventricular septum (IVS) mostly adjacent to the left ventricle (LV), in the embryonic heart (Fig. 1a–d) the expression of Adamts4 is more widespread throughout the left and right auricles (RA, LA), ventricles (LV and RV) and the inter-ventricular septum (IVS) of the chamber myocardium of E10.5, E12.5, E14.5, and E18.5 although its expression in endothelial-derived heart valves remained mostly inconspicuous. Further, the expression of Adamts4 at E13.5 (Fig. 1f) is also co-localized with cardiomyocyte-specific marker MF20 (MF20 is a myosin heavy chain-II marker in cardiac and skeletal muscle system, hence often used to label sections of myocardium and is therefore considered to be cardiomyocyte marker as well^{21,22}.) throughout the LV of chamber myocardium.

Adamts4 reactivation in the ventricular chamber in the adult heart following injury in-vivo. While Adamts4 expression in adult murine hearts significantly waned in comparison to developing hearts, it is found that MI-induced adult murine heart shows significant reactivation of Adamts4 protein. IHC with anti-Adamts4 antibody shows a strong expression of Adamts4 in the infarct and border zone (Fig. 2a) fol-

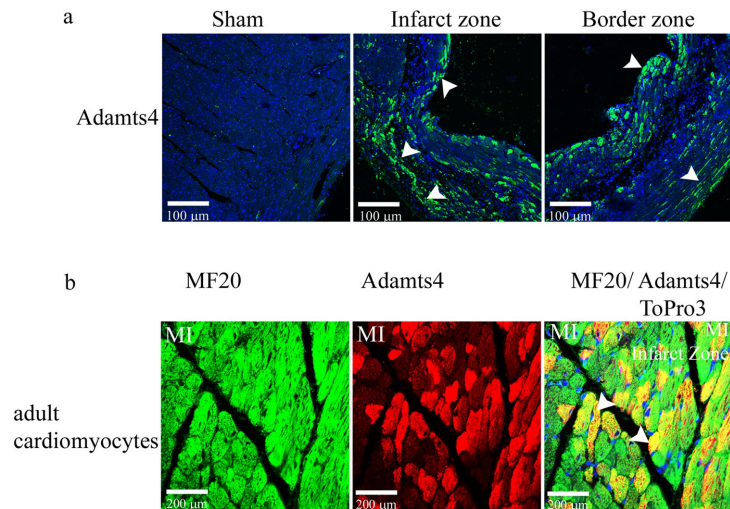


Figure 2. Adamts4 protein is reactivated in adult murine heart following 4 weeks post-MI. Panel a. shows IHC with anti-Adamts4 antibody (shown in green colour) and Topro3, used as nuclear stain (shown in blue). 4 weeks post-MI, induced reactivation of murine Adamts4, as indicated by the arrowheads in the infarct and border zones of adult murine chamber myocardium in comparison to sham operated mice. Moreover, this injury induced expression of Adamts4 is expressed in cardiomyocytes as shown in panel b where IHC with anti-Adamts4 (shown in red colour) and cardiomyocyte specific anti-MF20 (shown in green colour) antibodies following 4 weeks post MI in adult murine show colocalized expression, the colocalization is pointed out by the arrowheads in the MF20/Adamts4/Topro3 merged image. $n = 4$.

lowing 4 weeks post-MI in comparison to sham-operated mice. Again, this reactivated expression of Adamts4 following MI in adult mice is co-localized with MF20 as denoted by IHC with Adamts4 and MF20 (Fig. 2b) emphasizing that Adamts4 expression co-localizes with cardiomyocytes in adult hearts.

Adamts4, Tgf- β 1 upregulation in H9c2 cells following injury induction. To better understand the detailed mechanistic insights into Adamts4 function in post injury; further studies were done in H9c2, a rat cardiomyocyte cell line. H9c2 cells were subjected to H_2O_2 and Hypoxia (Hyp) treatment. Figure 3a, b show upregulation of ROS and hypoxia injury-related markers Catalase²³⁻²⁵ and Hif-1 α ²⁶ respectively validated by real-time qPCR, showing upregulation after injury for both the markers. Also, Adamts4 and Collagen-III^{27,28} expression at mRNA levels shows elevation after both stress treatments (Fig. 3c, d). Furthermore, Tgf- β 1 mRNA shows upregulation following H_2O_2 and Hypoxia treatment^{18,29} as quantified by real-time PCR (Fig. 3e). Moreover, Adamts4, α -SMA and Vimentin (a type-III intermediate filament marker that is known to induce repair mesenchymal cells following severe stress or injury to cells to initiate wound healing and provide structural support network^{30,31}) expression at protein levels assessed by western blot (WB) shows significant upregulation following H_2O_2 and Hypoxia treatments (Fig. 3f–i). Figure 3j depicts H9c2 morphology after injury induction as compared to control taken in DIC mode and cell size measurements post injury induction is shown in Supplementary Fig. S1. Overall, this figure shows the upregulation of ECM markers like Col-III, α -SMA, Vimentin along with Adamts4 and Tgf- β 1 following H_2O_2 and Hypoxia treatment. All qPCRs were normalized with β -actin and total protein was used as loading control for western blot assays.

Adamts4 and Tgf- β 1 expression is suppressed by SB431542 (ALKI) pre-treatment before H_2O_2 and Hypoxia stress induction. Immunofluorescence (IF) staining with anti-Adamts4 and anti-Tgf- β 1 antibody shows an elevated expression of both the markers following H_2O_2 and Hypoxia treatment assessed by quantifying fluorescence mean intensity (via ImageJ software, NIH). Interestingly, this elevated expression significantly reduced for both Adamts4 and Tgf- β 1 in presence of ALKI pre-treatment. Interesting to note, a non-specific nuclear presence of Adamts4 is observed irrespective of treatment (Fig. 4a–c) Further, the WB also shows a similar trend in the expression pattern of Adamts4 and Tgf- β 1 proteins where the expression of both markers falls after ALKI pre-treatment in comparison to only injury groups (Fig. 4d, e, g and h). Also, Tgf- β 1 measured at mRNA levels by qPCR also validates the same finding (Fig. 4f). Overall, ALKI shows successful significant inhibition of Tgf- β 1 as also stated previously^{20,32,33} along with inhibition of Adamts4. This finding is indicative of Tgf- β 1 dependent activation of Adamts4.

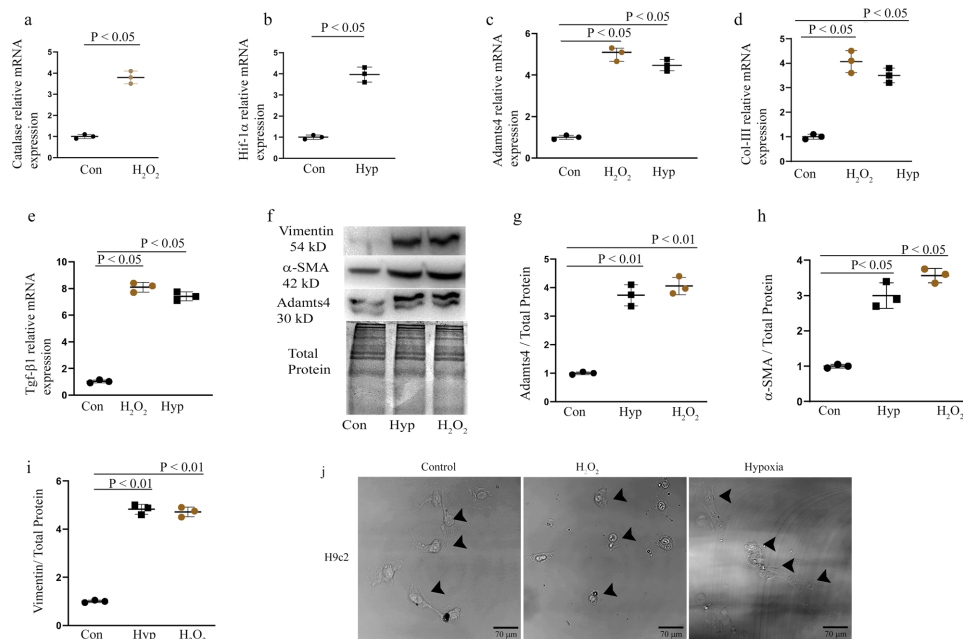


Figure 3. Injury induced overexpression of Adams4 and fibrosis related markers in H9c2 cells. Relative mRNA expression assessed by quantitative real-time PCRs of Catalase (a) shows an upregulation by 3.8 fold, Hif-1 α (b) was found to be elevated by fourfold, Adams4 (c) was found to be upregulated by 5 and 4.5 fold for H₂O₂ and Hyp treatment sets respectively, Col-III (d) was found to be elevated by 4 and 3.5 fold H₂O₂ and Hyp treatments, Tgf- β 1 (e) levels were upregulated by 8 and 7.4 folds for H₂O₂ and Hyp treatments respectively. Also, elevated expression of proteins analyzed by WB with Adams4 (f and g) showed an enhanced expression of 3.7 and fourfold for Hyp and H₂O₂ treatments, α -SMA (f and h) showed an upregulation of 3 and 3.5 folds Hyp and H₂O₂ treatment groups, Vimentin (f and i) under stress induced conditions of hypoxia and H₂O₂ showed upregulated expression by 4.8 fold for hypoxia and 4.7 fold for H₂O₂ treatments. Elevated expression of markers-Catalase and Hif-1 α signified successful injury inductions while upregulated expressions of Adams4, Col-III, Tgf- β 1, α -SMA and Vimentin indicated development of injury related fibrosis. β -actin was used to normalize gene expression for qPCR assay and total protein was used as loading control for WB. n = 3. Data analyzed and expressed as mean \pm SD. Differences were considered statistically significant for $p < 0.05$. (j) H9c2 morphology after injury induction as compared to control taken with the help of a DIC microscope.

ALKI pre-treatment before H₂O₂ and Hypoxia treatment suppresses the expression of Collagen-III and α -SMA. Fibrosis markers Collagen-III (Col-III) and α -SMA^{27,34,35} IF staining show a reduction in expression of both markers in H₂O₂ and Hyp groups pre-treated with ALKI after a significant upregulation in the expression of both markers observed in the injury groups; H₂O₂ and Hyp as measured by assessing fluorescence intensities of Col-III and α -SMA (Fig. 5a–c). Overall, this suggests that the expression of Collagen-III and α -SMA may be Adams4 and Tgf- β 1 dependent.

ALKI pre-treatment prior to H₂O₂ and Hypoxia treatment inhibits Periostin expression. Periostin expression is detected by IF staining with anti-Periostin antibody and shows upregulation of the same following H₂O₂ and Hyp treatments group in comparison to the control set but this elevation is significantly reduced in ALKI + H₂O₂ and ALKI + Hyp groups respectively in comparison to the control group (Fig. 6a, b). Adams4 loss of function mediated by Adams4 siRNA transfection (ATSSi Tr) was validated by WB (Fig. 6c, d), IF (Fig. 6e, f) and qPCR (Fig. 6g), all of which validated successful knockdown of Adams4 compared to the scrambled siRNA (Scsi Tr) treated group. Overall, these data suggest that Periostin activity may be Adams4 and Tgf- β 1 dependent.

Adams4 siRNA mediated gene knockdown before H₂O₂ and Hypoxia treatment inhibits Adams4 but does not affect Tgf- β 1 expression. Now to better understand the regulatory hierarchy and interaction between Tgf- β signaling and Adams4; Adams4 knockdown experiments are performed.

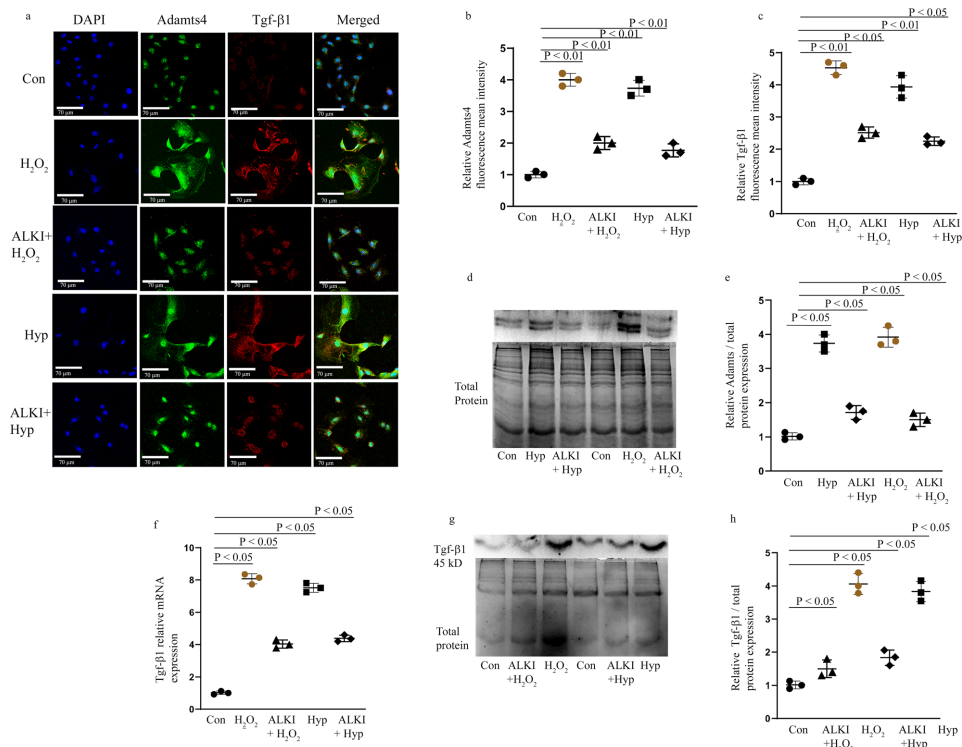


Figure 4. Adams4 and Tgf-β1 expression is inhibited following pre-treatment with ALKI. Staining with anti-Adams4 (shown in green) showed a 4- and 3.7-fold increase following H₂O₂ and hypoxia treatments in the fluorescence intensities of Adams4 but was found to reduce to 2 and 1.6 folds in the treatment groups—ALKI + H₂O₂ and ALKI + Hypoxia respectively (a and b). IF with anti-Tgf-β1 antibody (shown in red) showed elevated expression of 4.5 and fourfold following H₂O₂ and hypoxia treatments and this reduced to 2.5 and 2.3 folds for ALKI + H₂O₂ and ALKI + Hypoxia groups (a and c). DAPI (in blue) was used as nuclear stain. Adams4 WB shows of increased expression of 3.7 and 4 folds for the Hyp, H₂O₂ treated groups which reduce to 1.7, and 1.5 in ALKI + Hyp and ALKI + H₂O₂ treated groups (d and e). Tgf-β1 inhibition following ALKI pre-treatment was also assessed by qPCR (f) which showed a reduction from 8 and 7.4 folds for H₂O₂ and hypoxia treatment groups to 4 and 4.4 folds for ALKI + H₂O₂ and ALKI + Hyp treatment groups. Tgf-β1 protein expression measured by WB (g and h) showed a 4- and 3.8-fold increased change for H₂O₂ and Hypoxia subjected H9c2 cells to 1.5 and 1.8 folds for ALKI + H₂O₂ and ALKI + Hyp treatment respectively. β-actin was used to normalize gene expression for qPCR assay and total protein was used as loading control for WB. n = 3, data analyzed and expressed as mean ± SD. Differences were considered statistically significant for p < 0.05.

As expected, Adams4 siRNA transfection before H₂O₂ (ATssi + H₂O₂) and hypoxia (ATssi + Hyp) treatment show a significant reduction in the levels of Adams4 expression as shown by Adams4 IF staining (Fig. 7a, b) as compared to the treatment groups; H₂O₂ and Hyp, but interestingly Tgf-β1 expression (Fig. 7a, c) remains mostly unaffected by Adams4 loss of function as no significant difference between H₂O₂ and ATssi + H₂O₂ and Hyp and ATssi + Hyp was found. This finding, therefore, is suggestive of a possible Tgf-β1 function upstream of Adams4 at least in the context of H₂O₂ and hypoxia induced pathological remodeling in cultured H9c2 cells.

Adams4 knockdown results in inhibition of Collagen-III and α-SMA expression. Further, markers for injury induced fibrosis or pathological remodeling are determined in Adams4 dependent manner. Likewise, Adams4 siRNA mediated knockdown also shows a significant reduction in the expression of Collagen-III and α-SMA in groups where Adams4 knockdown was performed prior to H₂O₂ and hypoxia induction as compared to groups where only injury induction (H₂O₂ and hypoxia) was done, shown by Collagen-III and α-SMA IF staining (Fig. 8a–c). Overall, these findings are indicative of an Adams4 dependent activity under pathological stress conditions induced in H9c2 cells.

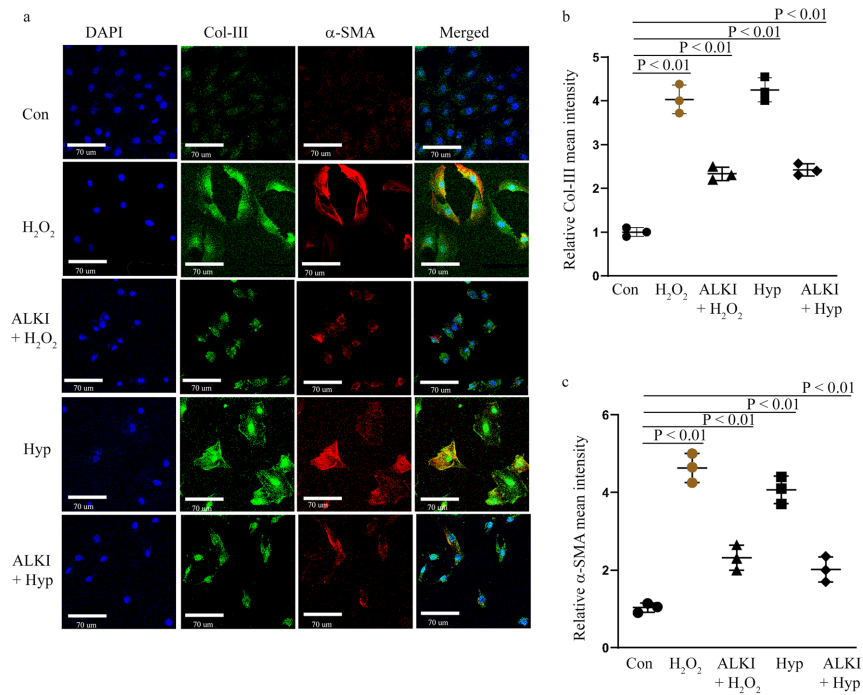


Figure 5. Inhibition of Col-III and α -SMA by ALKI pre-treatment. IF staining with anti-Col-III (shown in green) and anti- α -SMA (shown on red) antibodies showed inhibited expression of the markers under conditions of ALKI pre-treatment paired with H₂O₂ and hypoxia when compared to only injury states-H₂O₂ and hypoxia. Col-III expression reduced to 2.3 and 2.4 folds for ALKI+H₂O₂ and ALKI+ Hypoxia treatment sets from 4 and 4.25 folds for H₂O₂ and Hyp treatments respectively (a and b). α -SMA levels were reduced to 2.3 and 2 folds for ALKI+H₂O₂ and ALKI+ Hypoxia treatment groups from 4.6 and 4 folds for H₂O₂ and Hyp treatments respectively. DAPI (shown in blue) was used as nuclear stain n = 3, data analyzed and expressed as mean \pm SD. Differences were considered statistically significant for p < 0.05.

Adams4 knockdown results in reduced expression of Periostin. Moving along on the same lines as with ALKI treatment, next Periostin expression is detected by IF staining with anti-Periostin antibody post Adams4 knockdown and this shows upregulated expression of Periostin in H₂O₂ and Hyp treated groups in comparison to the control set, this elevation is significantly reduced in ATSSi+H₂O₂ and ATSSi+Hyp groups (Fig. 9a, b) showing a significant reduction from only H₂O₂ and Hyp treated H9c2 cells. These findings are indicative that Periostin expression may be under Adams4 regulation.

The induced expression of Adams4 and α -SMA in humans with cardiac anomalies. To better correlate our in vivo murine animal model and in vitro findings, in humans, we have used human patients' serum samples with indicated cardiac anomalies. Adams4 and α -SMA protein levels were assessed by western blot. Both Adams4 and α -SMA proteins show significantly enhanced expression in patients who have suffered DCM, MI, either AWTMI (anterior wall MI) or inferior wall MI (IWTMI) (Fig. 10a–c) Furthermore, Adams4 specific ELISA also validates the same findings (Fig. 10d). Patients with DCM, IWTMI or AWTMI show significant expression of Adams4 as compared to the control group. This confirms that Adams4 is also induced in humans who have a history of cardiac diseases like DCM or have suffered MI. Figure 10e shows a proposed model based on our findings for the interaction and inter-relationship between Adams4 and Tgf- β 1 in post cardiac injury conditions; when the Tgf- β 1 expression is inhibited by blocking the binding of Tgf- β 1 to one of its two binding receptors (ALK receptors, more specifically ALK 4 and 5), Adams4 expression is inhibited since it is regulated downstream of Tgf- β 1. So, the elevated fibrosis like conditions that escalated following pathological stress induction is inhibited and eventually fibrosis related markers (Col-III, α -SMA and periostin) along with Adams4 are downregulated following inhibition of Adams4.

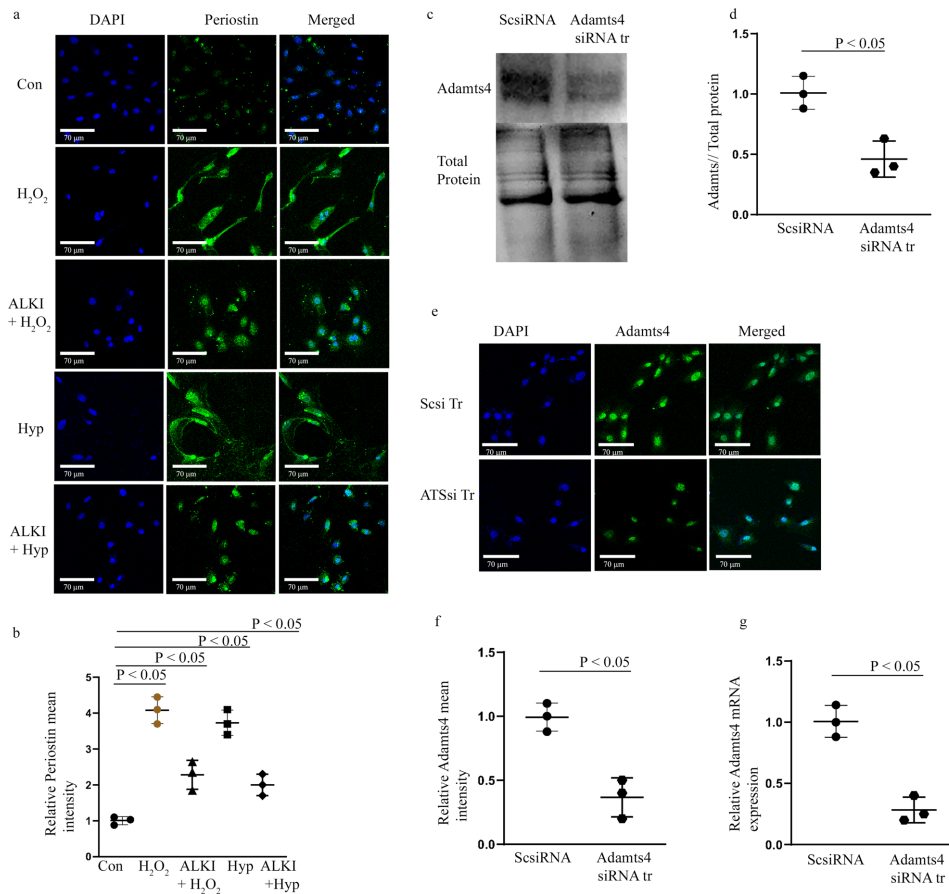


Figure 6. Periostin expression is reduced after ALKI pre-treatment and successful knockdown of Adamts4 mRNA in cultured H9c2 cells. IF with anti-Periostin antibody (shown in green) shows inhibition of Periostin expression under ALKI + H₂O₂, and ALKI + Hyp conditions as compared to only H₂O₂ and Hyp treated conditions. A reduced expression of 2.3 and 2 folds for ALKI + H₂O₂, and ALKI + Hyp was observed which was a decrease from the 4 and 3.7 fold change found for only H₂O₂ and Hyp treatments (a and b) in comparison to control. Successful knockdown of Adamts4 via Adamts4 siRNA transfection is shown by Adamts4 WB (shown in c and d), a 0.46 fold expression in the knockdown group against the control group was found. Further, Adamts4 IF (shown in green) also validated the successful knockdown of Adamts4. A decrease in the mean fluorescence intensity from 1 as observed for Scsi treatment set to 0.33 for ATSi tr group was found. (e and f). DAPI (shown in blue) was used as nuclear stain. Finally, from qPCR Adamts4 mRNA levels were downregulated from one fold observed for Scsi tr set to 0.25-fold for ATSi tr group (g). n = 3, data analyzed and expressed as mean ± SD. Differences were considered statistically significant for p < 0.05.

Discussion

The salient finding of this study is that Adamts4 is upregulated in injury to cardiac muscle. This finding is consistent with previous studies where Adamts4 expression was shown to be enhanced in atherosclerotic plaques¹³ and patients with acute coronary syndrome¹⁵. Importantly, Adamts4 being a secretory protein in nature, it resides both intracellularly and is also secreted from cardiomyocytes out into the ECM where its function is to regulate the turnover of other proteins by directly affecting other resident cells including but not limited to cardiac fibroblasts, endothelial and smooth muscle cells in the same ECM milieu. However, injury induced function of Adamts4 in other adult cardiac resident cell types is unknown. The expression of Adamts4 significantly

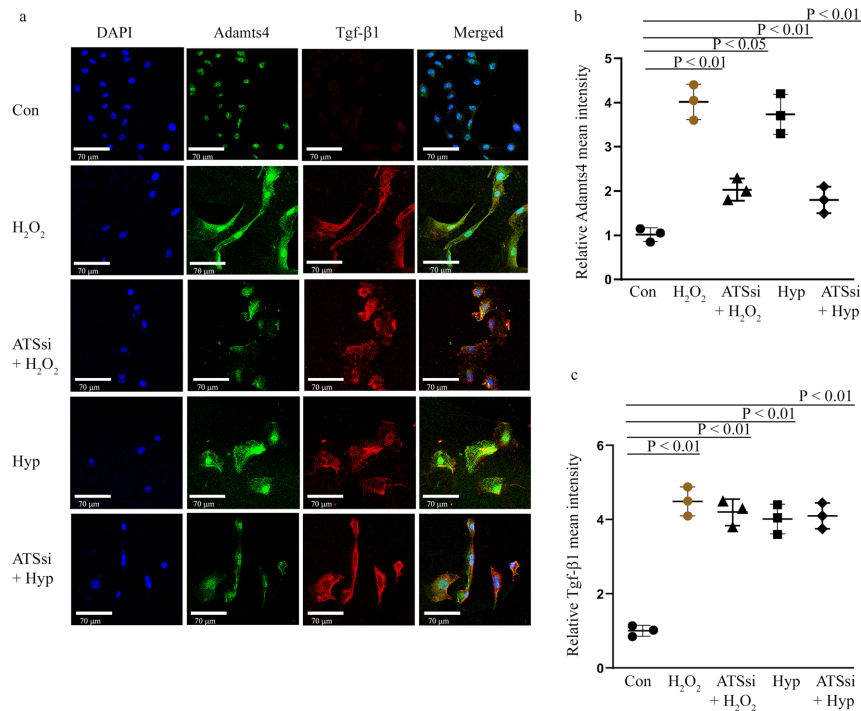


Figure 7. Tgf-β1 expression remains unaffected by Adamts4 knockdown. IF with anti-Adamts4 (shown in green) showed downregulation of Adamts4 following Adamts4 loss of function along with injury treatments. Adamts4 levels were found to decrease to 2 and 1.8 folds in the ATSSi + H₂O₂ and ATSSi + Hyp groups in comparison to the 4 and 3.7 folds increase observed for only H₂O₂ and Hyp treatments (a and b) but Tgf-β1 remained largely unaffected by this loss of function of Adamts4 and as shown by staining with anti-Tgf-β1 (shown in red) where the levels of Tgf-β1 were 4.5 and 4.0 for H₂O₂ and Hyp groups and 4.2 and 4.1 for ATSSi + H₂O₂ and ATSSi + Hyp groups (a and c). DAPI (shown in blue) was used as nuclear stain. Differences between groups H₂O₂ and ATSSi + H₂O₂, and Hyp and ATSSi + Hyp were not found to be significant. n = 3, data analyzed and expressed as mean ± SD. Differences were considered statistically significant for p < 0.05.

decreased from being widespread in the chamber myocardium of developing hearts to very restricted expression in normal adult hearts (Fig. 1) which could imply that its roles in developing and adult hearts are different but the reactivation of Adamts4 following cardiac injury (MI) (Fig. 2) implied that it could be another marker for adult cardiac injury. Since, this expression co-localized with cardiomyocytes, manipulation of Adamts4 was easier to experiment with within H9c2, a cardiomyocyte cell line. Injury inductions through H₂O₂ and hypoxia treatment showed upregulation of Adamts4 along with a couple of other fibrosis-related markers like Tgf-β1, Collagen-III, α-SMA, and Periostin which is notably known as a marker for detecting fibroblast to myofibroblast switch³⁶ were found to be elevated (Figs. 3 and 6) implying that an injury mediated ECM remodeling could be a cause for the elevation of these markers. Further pre-treatment with SB431542, an inhibitor of ALK4 and 5 (one of the two binding receptors of Tgf-β1) receptor that eventually leads to inhibition of Tgf-β1 also showed inhibition of Adamts4, this inhibition further extended to the expression of Collagen-III, α-SMA and Periostin proteins (Figs. 4, 5 and 6). To better understand the hierarchy supremacy between Adamts4 and Tgf-β1, Adamts4 loss of function study was mediated by Adamts4 siRNA transfection. In groups where Adamts4 knockdown was performed before stress induction, Tgf-β1 expression remained quite unaffected whereas the expression of the other 3 mentioned markers-Collagen-III, α-SMA, and Periostin along with Adamts4 was found to reduce to somewhat similar levels when ALKI pre-treatment with stress induction was done (Figs. 7, 8 and 9). These findings indicated that Adamts4 expression is mediated by Tgf-β1 and also that other ECM and fibrosis related markers including Col-III, α-SMA, and Periostin seem to be regulated by Adamts4 since loss of function of Adamts4 significantly inhibited the expression of these markers following injury to H9c2 cells. Finally, not only our marker of interest, Adamts4 but also α-SMA showed significantly enhanced expression in patients with MI and DCM injury (Fig. 10) indicating a cardiac fibrosis like condition following adult cardiac injury. Although

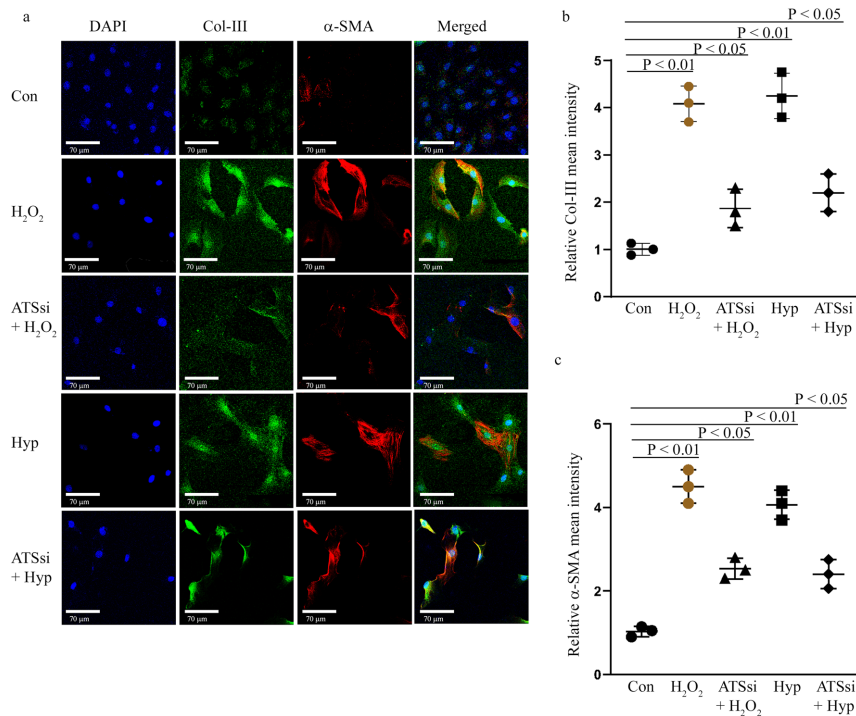


Figure 8. Inhibited expression of Col-III and α-SMA following loss of function of Adamts4. IF with anti-Col-III (shown in green) and anti-α-SMA (shown in red) antibodies show inhibited expression of these markers under ATSSi + H₂O₂ and ATSSi + Hyp conditions when compared with H₂O₂ and Hyp treated cells (a) Col-III showed a reduction from 4 and 4.25 fold observed for the H₂O₂ and Hyp treatment groups in comparison with the control group to 1.8 and 2.2 fold observed in ATSSi + H₂O₂ and ATSSi + Hyp groups (a and b). Similarly, for α-SMA, H₂O₂ and Hyp treated cells show a significant 4.5 and fourfold increased expression when compared to control, the ATSSi + H₂O₂ and ATSSi + Hyp treated cells show a fold change of 2.5 and 2.4 increments when compared to the control group (a and c). DAPI (shown in blue) was used as nuclear stain. n = 3, p < 0.05 is considered as significant for differences among groups. Data analysed and expressed as mean ± SD.

not done here but our future studies are focussed on validating the direct interaction of Adamts4 with Col-III α-SMA, and Periostin through binding/ChIP assays.

The ECM is an integral part of the myocardium. The dynamic composition of cardiac ECM consisting of both structural and non-structural components plays a critical role in cellular events and during pathogenicity^{37,38}. Under stress conditions such as Ischemia or MI, the chamber myocardium undergoes intensive ECM remodeling which remains relatively inconspicuous in healthy individuals. Cardiac Fibrosis is often viewed as an expansion of ECM remodelling³⁹. Following MI or I/R, there is an acute inflammatory response that suffices for the overexpression of pro-inflammatory cytokines like Tgf-β and interleukins. Tgf-β1 most notably does so by the canonical Smad 2/3 signaling cascade which leads to fibrosis^{16,17,39}. This, in turn, activates and synthesizes matrix macromolecule like Adamts^{40,41} family among others as a part of the pro-inflammatory mediated cell signaling cascade and these MMPs then take over the centre stage post-cardiac injury such as MI which leaves behind a pool of necrotic myocytes, it is then that the MMPs like Adamts4 takeover to regulate a turn-over in the synthesis of matrix macromolecules like Collagen-I/III, α-SMA, and Periostin, Tenascin-C to synthesize more matrix macromolecules and fibroblasts which is required to fill in the scar left by necrosis of myocardial cells in order to maintain the physiology of the myocardium since adult cardiomyocytes have very limited proliferation capacity. However, prolonged expansion of ECM could lead to extensive fibrosis and as a resulting stiffness of the myocardium following which ventricular dysfunction could occur which itself may turn fatal and thus inhibition of MMPs like Adamts4 could be one of the possible targets to reduce fibrosis post-cardiac injury⁴² like the one proposed in our model (Fig. 10e) by inhibiting Tgf-β1.

To conclude, Adamts4 is upregulated in response to cardiac stress in *in-vivo*, *in-vitro* and human studies, and this upregulation is mediated by Tgf-β1. This elevation of Adamts4 leads to fibrosis induction as markers related

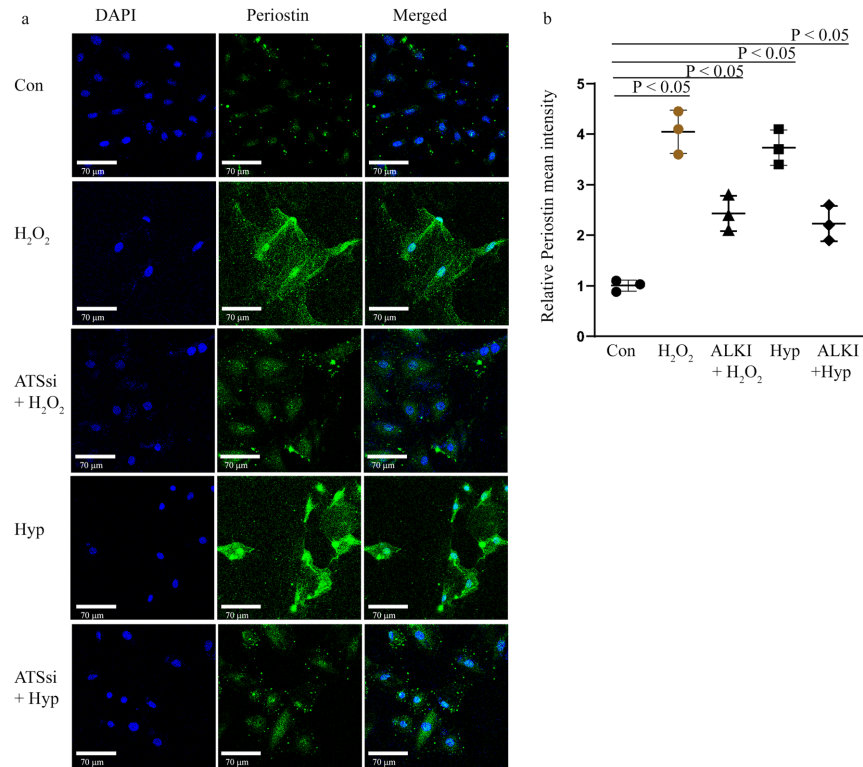


Figure 9. Reduced expression of Periostin following *Adams4* loss of function. IF with anti-Periostin antibody (shown in green colour) shows a fold change of 4 and 3.7 increase in the H₂O₂ and Hyp treated group in comparison to the control set, this elevation is significantly reduced 2.4 and 2.2 in ATSSi + H₂O₂ and ATSSi + Hyp groups following siRNA mediated knockdown of *Adams4* (a). DAPI (shown in blue) was used as nuclear stain. Its quantification is depicted in the graph (b). n = 3, data analysed and expressed as mean ± SD. Differences were considered statistically significant for p < 0.05.

to fibrosis including Collagen-III, α-SMA, and Periostin along with Tgf-β1 is also found to be upregulated but when *Adams4* loss of function is performed, these markers were also found to be inhibited following injury except for Tgf-β1 which remains unaffected indicating that it is upstream of *Adams4* in the signaling cascade. Our findings suggest that *Adams4* after being activated by Tgf-β1 under stress inducing conditions, mediates ECM remodeling and thereafter fibrosis through the functioning of Periostin and α-SMA as determined by our findings. It is possible that Periostin, another secretory ECM molecule known to either regulate or work in tandem with other MMPs^{43,44}, works in synchronisation with *Adams4* to regulate ECM remodeling and induce fibrosis. Our findings show an *Adams4* dependent Periostin functioning (depicted by *Adams4* loss of function assay) but to state whether *Adams4* and Periostin directly interact, requires further experimentation to establish any direct association between these two ECM molecules. α-SMA has been known to induce fibroblast contractility and is highly expressed in infarct myofibroblasts to prevent extreme remodeling and thereafter cardiac rupture^{45,46}. As our data shows the hallmark expression of *Adams4* in cardiac stress conditions, it can be considered as a novel biomarker for cardiac related injuries leading way for therapeutics to manipulate its expression following cardiac injury for improvement of cardiac functioning. Finally, our work hypothesises that *Adams4* being an ECM secretory protein, after being secreted from chamber myocardium regulates ECM and its remodeling, the details of this mechanism require further depth, understanding and experimentations.

Methods

Animal study and experimentation. All experiments involving animals were carried out with the experimental protocols and procedures reviewed and approved by the Cincinnati Children's Hospital Medical Center Biohazard Safety Committee and Institutional Animal Care and Use Committee. The study was per-

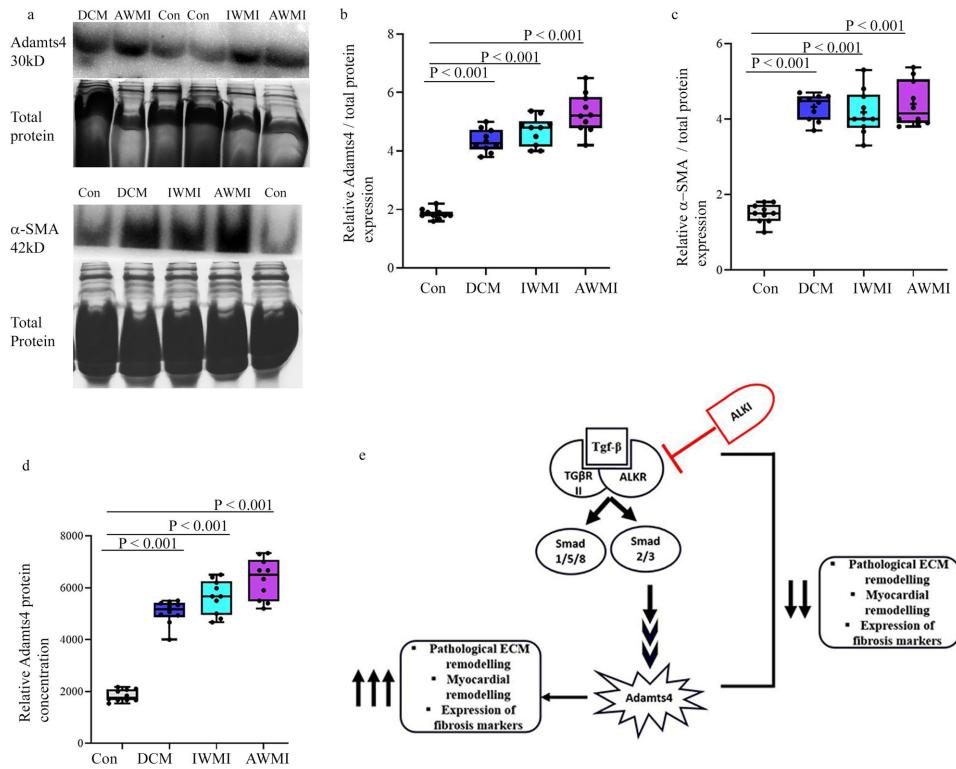


Figure 10. Upregulation of Adamts4 and α -SMA proteins in adult cardiac patients. Adamts4 and α -SMA WB data of affected cardiac patients and control (a), its quantification (b and c). An elevated expression of Adamts4 varying from 3 to 4.5 folds for patients with DCM, 4 to 5.3 folds for IWMI patients and 4 to 6.5 for patients with AWMI and varying in comparison to the control group (with no indicated cardiac abnormalities), where the expression fold varies from 1.6 to 2.3 fold. (a and b) was observed. The same was true for α -SMA which showed increased fold change varied from 3.7 to 4.7, 3.3 to 5.3, 3.9 to 5.4 for DCM, IWMI, and AWMI groups in comparison with the control set where fold levels for α -SMA varied from 1 to 1.8. (a and c). Total protein was used as loading control. Further, Adamts4 specific ELISA showed concentration gradient varying from 4666 to 6500 (pg/ml), 5200 to 7333 (pg/ml), and 4000 to 5500 (pg/ml) for DCM, IWMI, and AWMI groups respectively as compared to the concentration gradient observed for the control group which varied from 1533 to 2170 (pg/ml) (d). (n = 5 for WB for each group, N = 10 and n = 2 for ELISA for each study group). Data analyzed and expressed as median, 1st and 3rd quartile and range. $p < 0.05$ was considered a significant difference. The proposed model (e) shows the hypothetical hierarchy and inter-relationship between Tgf- β 1 and Adamts4 based on our findings. ALKI acting as an inhibitor of Tgf- β 1 inhibits the stimulation of Adamts4 by Tgf- β 1 which normally is activated under stress or injury conditions and activates downstream molecule Adamts4 and Adamts4 then proceeds with pathological ECM remodeling to restore the damaged physiology of the cells and tissues.

formed in accordance with ARRIVE guidelines and all animal experiments were conducted in compliance with the relevant guidelines. Timed-matings were established, with the morning of an observed copulation plug set at E0.5. For embryonic studies, whole embryos or hearts were harvested on E10.5, E12.5, E14.5, and E18.5 days and proceeded with IHC. For MI induction, 8–10 weeks old adult male Swiss albino mice were used. MI was performed as described previously²⁴.

Immunohistochemistry. Whole embryos and embryonic or adult hearts were harvested, washed in 1X PBS, fixed in 4% paraformaldehyde, dehydrated, and embedded in paraffin. Later the tissue sectioning (5–7 μ m) was done using a microtome (Leica Biosystems). For immunohistochemistry, the tissue sections were deparaffinized and hydrated after which antigen retrieval was done using citrate buffer (pH 6) washed in 1X PBS and thereafter, blocking solution (2% BSA with 0.1% Tween20) was added to the sections for 1 h. Later after blocking,

Groups	Control (n = 10)	DCM (n = 10)	AWMI (n = 10)	IWMI (10)
Age	20–55 years	20–55 years	28–60 years	30–60 years
Mean age	44 ± 2 years	43 ± 2 years	47 ± 2 years	47 ± 2 years
Sex, M/F	6/4	6/4	7/3	7/3
Smoker, M/F	0/0	3/0	4/0	1/1

Table 1. Characteristics of clinical sample groups.

the sections were incubated overnight at 4 °C. The following day, the incubated sections were washed in PBS and incubated with secondary antibodies against their respective primary antibodies. The sections were mounted using Vectashied (Vector Labs). The primary antibodies used were Adamts4 (PA1-1749A, Invitrogen), MF20 (1:200, DSHB), and respective secondary antibodies [anti-rabbit/mouse Alexa 488 (green; ab150077, Abcam) or 594 (red; ab150116, Abcam) fluorescent-conjugated; Molecular Probes, 1:100]. Topro3 (Molecular Probes, 1:1000) was used as a nuclear stain. Fluorescent images were acquired using a Zeiss LSM 510 confocal microscope and LSM version 3.2 SP2 software.

Human studies. A total of 30 affected clinical samples were used for this study. Venous blood samples were used for the study. The approval for the collection was ethically approved by the Institutional ethics committee of IPGME&R, Kolkata (IPGME&R/IEC/2019/517). All experiments were approved and performed according to the institutional guidelines of IPGME&R, Kolkata. Informed consent was obtained from all participants. Two broad categories of cardiac conditions were selected namely, Dilated cardiomyopathy (DCM), Myocardial Infarction (including AWMI-anterior wall MI and IWMI-inferior wall MI). MI patients routinely given Statin, high intensity, usually 80 mg of Atorvastatin. Loading doses of Aspirin 300 mg and Clopidogrel 300 mg along with Angiotensin Receptor Blocker (ARB) or Angiotensin Converting Enzyme Inhibitor (ACEI), β -Blocker, nitroglycerin, tranquilizer. DCM cases were given ACEI/ARB/Angiotensin Receptor Neprilysin Inhibitor (ARNI), SGLT2 inhibitors, β -blocker, diuretic, Mineralocorticoid Receptor Antagonist (MRA) and supportive therapy like O₂. Blood collection timing varied between 12 and 36 h of onset or hospitalisation. Control group consisted of blood collected from healthy volunteers who were not known to be diagnosed with any cardiac ailments or any other lifestyle disease for the record. The characteristics of the patient samples are provided in the following Table 1. Blood samples were obtained in clot vials. The serum was separated by following standard procedure by subjecting the clot vials to centrifugation at 2500 rpm for 10 min at 25 °C. To the isolated serum, protease inhibitor (Genetix GX-2811AR) and phosphatase inhibitor (Genetix GX-0211AR) were added according to the manufacturer's instructions and stored at –20 °C until further use for Western Blotting and ELISA.

Cell culture studies. All the *in-vitro* experiments were performed on H9c2, rat ventricular cardiomyoblast cell line. The cells were cultured in Dulbecco's modified Eagle's medium (AT007, Himedia) supplemented with 10% FBS (RM10409, Himedia) and 1% penicillin/streptomycin (Pen-Strep) cocktail (15140122, Invitrogen) maintained at a sterile humidified CO₂ incubator at 5% levels and 37 °C²³. The cells were used for further experiments at about 75–80% confluency. For experimental treatments, serum-free DMEM was used. For ROS generation, the cells were treated with H₂O₂ (100 μ M) for 1 h^{24,25}. For hypoxia induction, the cells were put in an anaerobic chamber with an anergas pack (LE200A, Himedia) and anaero indicator tablet (LE065, Himedia) according to the manufacturer's instructions. The anaerobic chamber with cells was incubated in the CO₂ incubator for 12 h, the indicator color change confirmed hypoxia induction in the chamber¹⁷.

TGF- β inhibitor SB431542 and siRNA treatment. For TGF- β inhibition, the cells were pre-treated with a potent ALK inhibitor, SB431542 (10 μ M) (ab120163, Abcam) for 30 min following which the cells were exposed to H₂O₂ and hypoxia induction as earlier mentioned²⁰. For knockdown of Adamts4, cells were transfected with Adamts4 siRNA (50 pmol) (4390771, Ambion) and Lipofectamine RNAiMax reagent (13778-075, Invitrogen) when the cells were at least 70% confluent for 48 h following manufacturer's protocol after overnight serum starvation. For negative control, scrambled siRNA (silence select negative control no 1 siRNA) (4390843, Ambion) was used similarly. After 48 h of Adamts4 siRNA treatment, the cells were subjected to H₂O₂ and hypoxia treatment as previously described.

RNA isolation, RT-PCR, and real-time PCR. Total RNA was isolated from control and treated H9c2 cells with Trizol (15596026, Ambion) following the Trizol-Chloroform method. Taking 1 μ g of total RNA isolated, cDNA was synthesized using Biorad cDNA synthesis kit (iScript™ Reverse Transcription Supermix for RT, 170-884) in 20 μ l of total volume according to manufacturer's supplied protocol. The cDNA prepared was used for primer optimization and standardization using DNA Taq polymerase (by RT-PCR in reverse time for real-time PCR against primers (BIOTAQ DNA polymerase BIO-21040, Bioline). The PCRs were performed for 35 cycles using 20 pmol of the rodent primer pairs: Adamts4 (F): 5'-TCATGAAGTGGCCATGTCT-3' and (R): 5'-GTCAGTGATGAATCGGGGCAC-3'; Hif-1 α (F): 5'-CCAGCAGACCCAGTTACAGA-3' and (R): 5'-TTCCTGCTGTGTGAG-3'; β -actin (F): 5'-TCTTCCAGCCCTTCTCTCTG-3' and (R): 5'-CACACAGAGTACTTGCGCTC-3' and Catalase (F): 5'-CCTCGTTCAGGATGTGGTTT-3' and (R): 5'-TCTGGTGATATC GTGGGTGA-3', Tgf- β 1 (F): 5'-CTGAACCAAGGAGACGGAATAC-3' and (R): 5'-CTCTGTGGAGCTGAA

GCAATAG-3' and Collagen-III (F): 5'-CTGGTCCTGTTGGTCCATCT-3' and (R): 5'-ACCTTTGTACCTCG TGGAC-3'. These primer pairs were further used for real-time PCR studies. Real-time PCR was performed using Bio-Rad real-time PCR kit (172-52 03AP, SSO fast Eva green super mix). The gene expression of the mentioned genes was normalized with β -actin.

Protein isolation and western blotting. Protein isolation was done using ice-cold mammalian lysis buffer (250 mM NaCl, 50 mM Tris pH 7.5, 0.1% SDS, 1% TritonX, and 5 mM EDTA) containing protease inhibitor cocktail (Genetix GX-2811AR) and phosphatase inhibitor (Genetix GX-0211AR). The proteins were stored in small aliquots at -80°C until further use for Western Blotting (WB). Western blotting was performed as previously described⁴⁸. The immunoblots developed using Clarity™ Western ECL substrate (1705060, Bio-Rad) and scanned using ChemiDocMP (Bio-Rad) as previously described⁴⁹. The antibodies used were Adamts4 (PA1-1749A, Invitrogen) used at a concentration of 2 $\mu\text{g}/\text{ml}$, α -SMA (14-976082, Invitrogen) used at a dilution of 1:500, Tgf- β 1 (ab64715, Abcam) used at a concentration of 1 $\mu\text{g}/\text{ml}$ and Vimentin (ab17321, Abcam) at a dilution of 1:1000. After overnight incubation at 4°C with these primary antibodies, the corresponding secondary antibodies-HRP conjugated secondary goat anti-rabbit (ab97051, Abcam) and HRP conjugated goat anti-mouse secondary antibodies (ab97023, Abcam) were added against their respective primary antibodies at a dilution of 1:3000. The SDS gels were also stained with 2.5% coomassie (Brilliant blue G, SRL) and destained with coomassie de-stainer to obtain total protein intensities. The coomassie stained gels were scanned using ChemiDoc MP mentioned earlier. Quantification of intensities was done using ImageJ software (NIH). Figures for unprocessed blots and gels are also included in Supplementary Figs. S5, S6, S7 and S8 with highlighted regions (in red box) corresponding to the data depicted in the main manuscript figures. Full-length blots could not be submitted since the blots were trimmed (according to molecular size of the proteins) before hybridisation with respective antibodies to save on the antibodies and reagents.

Immunostaining. Immunostaining was performed in H9c2 cells following the protocol previously described²⁵ except for the omission of permeabilization steps for staining with antibodies. Adamts4 (PA1-1749A, Invitrogen) used as mentioned earlier, Tgf- β 1 (ab 64715, Abcam) used at a concentration of 2 $\mu\text{g}/\text{ml}$, α -SMA (14-976082, Invitrogen) used at 1:400 dilution, collagen III (ab 7778, Abcam) at a dilution of 1:1000 and Periostin (ab14041, Abcam) used at a dilution of 1:500. After overnight incubation at 4°C with these primary antibodies, the corresponding secondary antibodies Alexa flour 488 goat anti-rabbit secondary antibody (ab150077, Abcam) and Alexa flour 594 goat anti-mouse secondary antibody (ab150116, Abcam) were added against their respective primary antibodies. All cell nuclei were stained with DAPI (D9542, Sigma). Images were acquired using Leica confocal microscope and LasX software. The fluorescence intensities were measured and quantified with the help of ImageJ software (NIH).

Enzyme linked immunosorbent assay (ELISA). ELISA kit (ab213753, Abcam) was used to perform ELISA. Serum proteins were diluted with sample buffer in the ratio of 1:10 and samples were loaded onto the wells in duplicates. ELISA was performed as stated by the manufacturer's protocol.

Statistical analysis. All the results are mostly represented as mean \pm Standard Deviation of mean (SD) or as median, quartiles and range (Fig. 10). Statistical analyses were done using student's unpaired two-tailed T-test and one-way ANOVA for more than 2 groups. GraphPad Prism 9.3.1 was used for statistical analysis. Differences among the groups were considered statistically significant for $P < 0.05$.

Data availability

All the generated data used to support the findings of this study are either included within the article or in the supplementary file.

Received: 10 June 2021; Accepted: 30 May 2022

Published online: 14 June 2022

References

- Bui, A. L., Horwich, T. B. & Fonarow, G. C. Epidemiology and risk profile of heart failure. *Nat. Rev. Cardiol.* **8**, 30–41 (2011).
- Srivastava, A. & Mohanty, S. K. Age and sex pattern of cardiovascular mortality, hospitalisation and associated cost in India. *PLoS ONE* **8**, 1–13 (2013).
- Prabhakaran, D. *et al.* Cardiovascular diseases in India compared with the United States. *J. Am. Coll. Cardiol.* **72**, 79–95 (2018).
- Dobaczewski, M., Gonzalez-Quesada, C. & Frangogiannis, N. G. The extracellular matrix as a modulator of the inflammatory and reparative response following myocardial infarction. *J. Mol. Cell. Cardiol.* **48**, 504–511 (2010).
- Levick, S. P. & Brower, G. L. Regulation of matrix metalloproteinases is at the heart of myocardial remodeling. *Am. J. Physiol. Heart Circ. Physiol.* **295**, 8–10 (2018).
- Vistnes, M. *et al.* Pentosan polysulfate decreases myocardial expression of the extracellular matrix enzyme ADAMTS4 and improves cardiac function in vivo in rats subjected to pressure overload by aortic banding. *PLoS ONE* **9**, 66 (2014).
- Dobaczewski, M., Gonzalez-quesada, C. & Frangogiannis, N. G. The extracellular matrix as a modulator of the inflammatory and reparative response following myocardial infarction. *J. Mol. Cell. Cardiol.* **48**, 504–511 (2010).
- Talman, V. & Ruskoaho, H. Cardiac fibrosis in myocardial infarction—from repair and remodeling to regeneration. *Cell Tissue Res.* **365**, 563–581 (2016).
- Berk, B. C., Fujiwara, K. & Lehoux, S. Review series ECM remodeling in hypertensive heart disease. *J. Clin. Investig.* **117**, 66 (2007).
- DeAgüero, L. *et al.* Altered protein levels in the isolated extracellular matrix of failing human hearts with dilated cardiomyopathy. *Cardiovasc. Pathol.* **26**, 12–20 (2017).

11. Spinale, G. F. & Wilbur, M. N. Matrix metalloproteinase therapy in heart failure. *Curr. Treat. Options Cardiovasc. Med.* **11**, 339–346 (2009).
12. Uluçay, S. *et al.* A novel association between TGF β 1 and ADAMTS4 in coronary artery disease: A new potential mechanism in the progression of atherosclerosis and diabetes. *Anadolu Kardiyol. Derg.* **15**, 823–829 (2015).
13. Hossain, Z., Poh, K. K., Hirohata, S. & Ogawa, H. Loss of ADAMTS4 reduces high fat diet-induced atherosclerosis and enhances plaque stability in. *Nat. Publ. Gr.* <https://doi.org/10.1038/srep31130> (2016).
14. Li, K. *et al.* Assessing serum levels of ADAMTS1 and ADAMTS4 as new biomarkers for patients with type a acute aortic dissection. *Med. Sci. Monit.* **23**, 3913–3922 (2017).
15. Zha, Y., Chen, Y., Xu, F. & Zhang, J. Elevated level of ADAMTS4 in plasma and peripheral monocytes from patients with acute coronary syndrome. *Clin Res Cardiol* **2010**, 781–786. <https://doi.org/10.1007/s00392-010-0183-1> (2010).
16. Walton, K. L., Johnson, K. E. & Harrison, C. A. Targeting TGF- β mediated SMAD signaling for the prevention of fibrosis. *Front. Pharmacol.* **8**, 66 (2017).
17. Pohlers, D. *et al.* TGF- β and fibrosis in different organs—molecular pathway imprints. *Biochim. Biophys. Acta Mol. Basis Dis.* **1792**, 746–756 (2009).
18. Lou, Z. *et al.* Upregulation of NOX2 and NOX4 Mediated by TGF- β signaling pathway exacerbates cerebral ischemia/reperfusion oxidative stress injury. *Cell. Physiol. Biochem.* **46**, 2103–2113 (2018).
19. Frangogiannis, N. G. Cardiac fibrosis: Cell biological mechanisms, molecular pathways and therapeutic opportunities. *Mol. Asp. Med.* **65**, 66 (2019).
20. Yang, Y. F., Wu, C. C., Chen, W. P. & Su, M. J. Transforming growth factor- β type I receptor/ALK5 contributes to doxazosin-induced apoptosis in H9c2 cells. *Naunyn. Schmiedeberg. Arch. Pharmacol.* **380**, 561–567 (2009).
21. López-Unzu, M. A., Durán, A. C., Soto-Navarrete, M. T., Sans-Coma, V. & Fernández, B. Differential expression of myosin heavy chain isoforms in cardiac segments of gnathostome vertebrates and its evolutionary implications. *Front. Zool.* **16**, 1–15 (2019).
22. Kokkinopoulos, I. *et al.* Cardiomyocyte differentiation from mouse embryonic stem cells using a simple and defined protocol. *Dev. Dyn.* **245**, 157–165 (2016).
23. Fernández-Rojas, B., Vázquez-Cervantes, G. I., Pedraza-Chaverri, J. & Gutiérrez-Venegas, G. Lipoteichoic acid reduces antioxidant enzymes in H9c2 cells. *Toxicol. Reports* **7**, 101–108 (2020).
24. Sengupta, A., Molkentin, J. D., Paik, J. H., DePinho, R. A. & Yutzey, K. E. FoxO transcription factors promote cardiomyocyte survival upon induction of oxidative stress. *J. Biol. Chem.* **286**, 7468–7478 (2011).
25. Sen, P., Polley, A., Sengupta, A. & Chakraborty, S. Tbx20 promotes H9c2 cell survival against oxidative stress and hypoxia in vitro. *Indian J. Exp. Biol.* **57**, 643–655 (2019).
26. Vukovic, V. *et al.* Hypoxia-inducible factor-1 α is an intrinsic marker for hypoxia in cervical cancer xenografts. *Cancer Res.* **61**, 7394–7398 (2001).
27. Gao, Y., Chu, M., Hong, J., Shang, J. & Xu, D. Hypoxia induces cardiac fibroblast proliferation and phenotypic switch: A role for caveolae and caveolin-1/PTEN mediated pathway. *J. Thorac. Dis.* **6**, 1458–1468 (2014).
28. Lijnen, P. J., van Pelt, J. F. & Fagard, R. H. Stimulation of reactive oxygen species and collagen synthesis by angiotensin II in cardiac fibroblasts. *Cardiovasc. Ther.* **30**, 1–8 (2012).
29. Liu, R. M. & Desai, L. P. Reciprocal regulation of TGF- β and reactive oxygen species: A perverse cycle for fibrosis. *Redox Biol.* **6**, 565–577 (2015).
30. Walker, J. L., Bleaken, B. M., Romisher, A. R., Alnwibit, A. A. & Menko, A. S. In wound repair vimentin mediates the transition of mesenchymal leader cells to a myofibroblast phenotype. *Mol. Biol. Cell* **29**, 1555–1570 (2018).
31. Rog-Zielinska, E. A., Norris, R. A., Kohl, P. & Markwald, R. The Living scar—Cardiac fibroblasts and the injured heart. *Trends Mol. Med.* **22**, 99–114 (2016).
32. Inman, G. J. *et al.* SB-431542 is a potent and specific inhibitor of transforming growth factor-beta superfamily type I activin receptor-like kinase (ALK) receptors ALK4, ALK5, and ALK7. *Mol. Pharmacol.* **62**, 65–74 (2002).
33. Halder, S. K., Beauchamp, R. D. & Datta, P. K. A specific inhibitor of TGF- β receptor kinase, SB-431542, as a potent antitumor agent for human cancers. *Neoplasia* **7**, 509–521 (2005).
34. Karsdal, M. A. *et al.* Collagen biology and non-invasive biomarkers of liver fibrosis. *Liver Int.* **40**, 736–750 (2020).
35. Hinderer, S. & Schenke-Layland, K. Cardiac fibrosis—A short review of causes and therapeutic strategies. *Adv. Drug Deliv. Rev.* **146**, 77–82 (2019).
36. Frangogiannis, N. G. The extracellular matrix in ischemic and nonischemic heart failure. *Circ. Res.* **125**, 117–146 (2019).
37. Rienks, M., Papageorgiou, A. P., Frangogiannis, N. G. & Heymans, S. Myocardial extracellular matrix: An ever-changing and diverse entity. *Circ. Res.* **114**, 872–888 (2014).
38. Miner, E. C. & Miller, W. L. A look between the cardiomyocytes: The extracellular matrix in heart failure. *Mayo Clin. Proc.* **81**, 71–76 (2006).
39. Frangogiannis, N. G. Cardiac fibrosis: Cell biological mechanisms, molecular pathways and therapeutic opportunities. *Mol. Asp. Med.* **65**, 70–99 (2019).
40. Rienks, M., Barallobre-Barreiro, J. & Mayr, M. The emerging role of the ADAMTS family in vascular diseases. *Circ. Res.* **123**, 1279–1281 (2018).
41. Perrucci, G. L., Rurali, E. & Pompilio, G. Cardiac fibrosis in regenerative medicine: Destroy to rebuild. *J. Thorac. Dis.* **10**, S2376–S2389 (2018).
42. Kapelko, V. I. Extracellular matrix alterations in cardiomyopathy: The possible crucial role in the dilative form. *Exp. Clin. Cardiol.* **6**, 41–49 (2001).
43. Chijimatsu, R. *et al.* Expression and pathological effects of periostin in human osteoarthritis cartilage. *BMC Musculoskelet. Disord.* **16**, 1–12 (2015).
44. Kudo, A. & Kii, I. Periostin function in communication with extracellular matrices. *J. Cell Commun. Signal.* **12**, 301–308 (2018).
45. Hinz, B., Celetta, G., Tomasek, J. J., Gabbiani, G. & Chaponnier, C. Alpha-smooth muscle actin expression upregulates fibroblast contractile activity. *Mol. Biol. Cell* **12**, 2730–2741 (2001).
46. Shinde, A. V., Humeres, C. & Frangogiannis, N. G. The role of α -smooth muscle actin in fibroblast-mediated matrix contraction and remodeling. *Biochim. Biophys. Acta Mol. Basis Dis.* **1863**, 298–309 (2017).
47. Ma, Y. *et al.* DPP-4 inhibitor anagliptin protects against hypoxia-induced cytotoxicity in cardiac H9c2 cells. *Artif. Cells Nanomed. Biotechnol.* **47**, 3823–3831 (2019).
48. Evans-Anderson, H. J., Alferi, C. M. & Yutzey, K. E. Regulation of cardiomyocyte proliferation and myocardial growth during development by FOXO transcription factors. *Circ. Res.* **102**, 686–694 (2008).
49. Polley, A., Khanam, R., Sengupta, A. & Chakraborty, S. Asporin reduces adult aortic valve interstitial cell mineralization induced by osteogenic media and Wnt signaling manipulation in vitro. *Int. J. Cell Biol.* **66**, 2020 (2020).

Acknowledgements

We thank Prof. Katherine E. Yutzey, Professor, The Heart Institute, Division of Molecular Cardiovascular Biology, Cincinnati Children's Hospital Medical Center, Cincinnati, Ohio, USA for her overall supervision and support for all the in vivo experimentations. This study was supported by the Council of Scientific and Industrial Research,

Central Government of India sponsored project grant [No. 37(1735)/19/EMR-II] and Science and Engineering Research Board, Department of Science and Technology, Central Government of India sponsored project grant (File no: EMR/2017/001382) to SC. We also like to acknowledge DBT-Builder Programme (No. BT/INF/22/SP45088/2022) and DST-FIST (level I, No. SR/FST/LSI-560/2013) for their generous funding and support to the Department of Life Sciences, Presidency University, Kolkata.

Author contributions

R.K. designed, executed all the in vitro and human sample experimental work, performed the statistical analysis and wrote the manuscript. A.S.G. performed the in vivo M.I., provided reagents and intellectual inputs. D.M. provided the samples and supervision for human studies. S.C. designed the experiments, performed all timed-matings and embryonic studies, provided reagents and conceived the study. All authors reviewed the manuscript.

Competing interests

The authors declare no competing interests.

Additional information

Supplementary Information The online version contains supplementary material available at <https://doi.org/10.1038/s41598-022-13918-3>.

Correspondence and requests for materials should be addressed to S.C.

Reprints and permissions information is available at www.nature.com/reprints.





Publisher's note Springer Nature remains neutral with regard to jurisdictional claims in published maps and institutional affiliations.



Open Access This article is licensed under a Creative Commons Attribution 4.0 International License, which permits use, sharing, adaptation, distribution and reproduction in any medium or format, as long as you give appropriate credit to the original author(s) and the source, provide a link to the Creative Commons licence, and indicate if changes were made. The images or other third party material in this article are included in the article's Creative Commons licence, unless indicated otherwise in a credit line to the material. If material is not included in the article's Creative Commons licence and your intended use is not permitted by statutory regulation or exceeds the permitted use, you will need to obtain permission directly from the copyright holder. To view a copy of this licence, visit <http://creativecommons.org/licenses/by/4.0/>.

© The Author(s) 2022

Conference & seminar certificates

	XLII ALL INDIA CELL BIOLOGY CONFERENCE and 2 ND International Conference on TRENDS IN CELL AND MOLECULAR BIOLOGY December 21 - 23, 2018	
CERTIFICATE		
This is to certify that Prof./Dr./Mr./Ms. <u>RIFPAT KHANAM</u> of <u>PRESIDENCY UNIVERSITY, KOLKATA</u>		
has participated in the XLII All India Cell Biology Conference.		
He/she has presented a paper entitled " <u>Tox20 function in starvation induced autophagy in cultured Hec2 cells</u> " in oral /poster session of the conference.		
 Prof. Pradeep K. Burma Secretary, ISCB	 Dr. Angshuman Sarkar Convener	



Department of Zoology, University of Calcutta

INTZOOCON 2018

an International Conference to celebrate 100 years of excellence from 1919-2019
at the

Ramakrishna Mission Institute of Culture
& University of Calcutta (Ballygunge Campus)

February 1-3, 2018

Certificate of appreciation

This to certify that Prof./Dr./Mr./Mrs./Ms... *Riffat Khanam*

.....
participated in the International Conference as a Delegate/
Presenter of a Paper entitled *Injury induced Tbx20 function*
in cultured cardiac H9c2 cells.

Parthiba Basu
Sagartirtha Sarkar
Parthiba Basu & Sagartirtha Sarkar
Jt. Secretaries

Urmi Chatterji
Urmi Chatterji
President

**UGC-SAP (DRS II) Sponsored National Conference on
Stress Responses and Diseases (SR&D)**



06TH & 07TH MARCH, 2020

ORGANIZED BY

DEPARTMENT OF BIOCHEMISTRY AND BIOPHYSICS, UNIVERSITY OF KALYANI

*This is to certify that Prof./Dr./Mr./Mrs./Ms.....**Riffat Khanam**.....
participated in the UGC-SAP (DRS II) sponsored National Conference on SR&D, as
Invited Speaker/Presenter of an Abstract (Oral/Speed Talk/Poster)
/Organiser/Participant held on 06th and 7th March, 2020 at the Department of
Biochemistry and Biophysics, University of Kalyani, West Bengal.*


Dr. Angshuman Bagchi
Joint Convener


Prof. Tapati Chakraborti
HOD, Dept. of Biochem. & Biophys.


Dr. Jishu Naskar
Joint Convener



NUS
National University
of Singapore



Department of Biological Sciences

**26th Biological Sciences
Graduate Congress | 2021**
CONQUERING THE WAVES!



CERTIFICATE

Of Participation

This certificate is awarded to

Riffat Khanam

for delivering an Oral Presentation at the 26th Biological Sciences Graduate Congress
14 - 16 December 2021


Foo Sze Hui
Chairman
Organising Committee




Dr. Huang Danwei
Assistant Professor, NUS
Advisor, Biological Sciences Graduate
Congress

CERTIFICATE

OF PARTICIPATION

Cardiovascular Research Convergence 2022

This is to certify that Dr./Mr./Ms.

..... *Riffat.....Khanam*..... has participated

in Poster Presentation & won Third place in the Cardiovascular Research Convergence 2022, held on 25th June 2022 at CSIR-IICB, Kolkata.

Arun Bandyopadhyay

Dr. Arun Bandyopadhyay
Chairman, CRC 2022

Partha Chakrabarti

Dr. Partha Chakrabarti and Sanjay K Banerjee
Convenors, CRC-2022

Sanjay Banerjee

Prof. Sandeep Seth
Chief Editor, JPCS





Department of Biochemistry
University of Kashmir (NAAC Accredited A⁺)



Indian Society of Cell Biology
44th All India Cell Biology Conference & International Symposium on
Molecular & Cellular Insights of Human Diseases

Certificate of Achievement

This is to certify that

Mr. / Ms. Riffat Khanam is awarded

PROF. S. R. V. RAO AWARD

for the best Presentation in Oral/Poster Session,
held at the University of Kashmir, Srinagar from September 2-3, 2022.

Dr. Shajrul Amin
 Convener

Dr. Shaista Andrabi
 Organizing Secretary

Prof. Bhupendra N Singh
 Secretary ISCB